Spring 4-12-2018

Reducing Stress in 3D printed parts made with Laser Engineered Net Shaping

Shaun Ross Whetten

Shaun Whetten

Candidate

Mechanical Engineering

Department

This thesis is approved, and it is acceptable in quality and form for publication:

Approved by the Thesis Committee:

Yu-Lin Shen, Chairperson

Mehran Tehrani

David Keicher

Reducing Stress in 3D printed parts made with Laser Engineered Net Shaping

By

Shaun R. Whetten

B.S., Mechanical Engineering, University of New Mexico, 2016

THESIS

Submitted in partial fulfillment of the

Requirements for the Degree of

Masters of Science

Mechanical Engineering

University of New Mexico

Albuquerque, New Mexico

May 2018

II

Dedication

To my wife and children

Sarah Whetten

Max Whetten

Mia Whetten

Emi Whetten

I love you guys!!!

Acknowledgements

To start off I would like to acknowledge my loving wife Sarah, for her unending love and support during these years of my scholastic endeavors. You have been a support that is unmatched, and have always been willing to take on more than your fair share of responsibilities to make my load a little lighter. Thank you!! To Max, Mia, and Emi, thank you for being so understanding when I must cut play time short, to get my homework or other responsibilities taken care of. To the rest of my family, especially my parents Ross and Susan, for teaching me that I could accomplish anything that I set my mind to if I will just put my mind to it, and work hard.

I would also like to acknowledge my many friends and colleagues at Sandia National Laboratories for unending mentorship and support. A special thanks to Sita Mani, Judith Lavin, Andrew Kustas, Joe Bishop, and Adam Cook for priceless advice, guidance, and assistance. Each of your personal contributions to the success of my work have been greatly appreciated.

Without the support of my committee members, this thesis would not have been possible. I would like to thank Dr. Yu-Lin Shen for welcoming me into his research group, always being willing to answer my questions, Dr. Mehran Tehrani for his service an input on my committee, and David Keicher my long-term mentor and friend. Dave, you have given me a perspective and set of tools that I will take with me for the rest of my life. Always remember “Life is Good!!” Thank you for your support and inspiration.

Reducing Stress in 3D printed parts made with Laser Engineered Net Shaping

By

Shaun R. Whetten

B.S., Mechanical Engineering, University of New Mexico, 2016
M.S., Mechanical Engineering, University of New Mexico, 2018

ABSTRACT

Thermal cycling and repeated melting/solidification cycles characteristic of 3D metal printing processes causes buildup of residual stress in 3D printed parts. Using laser engineered net shaping (LENS®), residual stresses are formed leading to deformation and possible cracking of the 3D printed metal components. The LENS process offers opportunities for rapid prototyping, alternative manufacturing processes, and repair of worn/broken components so it is important to be able to minimize the effects of residual stress. Work was performed to understand the benefit of substrate heating on reducing residual stress in metal parts made using the LENS process. Substrate deformation, and destructive methods are used to determine residual stress at various levels of bed heating. Components printed at a range of heated bed temperatures will be compared, simulations that demonstrate the effects of the heating will be shown, and results will be discussed.

Table of Contents

List of Figures

List of Tables

Chapter 1 Introduction

1.1 Statement of Research

Additive manufacturing offers the unique ability to print prototype and production parts directly using CAD solid models. Even though many additive manufacturing (AM) technologies have been around since the 1990's or earlier, in recent years this field has experienced exponential growth [1]. Despite the advances AM has experienced in recent years, many of the technologies still have obstacles that need to be overcome. One problem that is prevalent in all laser based metallic additive manufacturing technologies is residual stress. One such process, Laser Engineered Net Shaping (LENS®), causes the material to be melted and re-melted repeatedly as a part is printed. The rapid heating and cooling associated with the re-melting causes repeated thermal cycling of the 3D printed part. The localized thermal cycling is a primary contributor to the development of non-uniform stress and strain fields [2]. The residual stress contained in the 3D printed components has a significant effect on the mechanical properties of the parts including: corrosion, fracture resistance, and fatigue performance [2]. Previous research suggests that temperature variations between the

core and outside edges of a component cause a large portion of its residual stress. This same research also show that another primary contributor to residual stress is the high cooling rate that the material experiences as it quenches from a molten liquid to solid [3]. The stresses found in 3d printed metal LENS parts are large enough to cause distortion, warping and cracking of the parts. Since the LENS process can also be used to repair existing hardware, part distortion due to residual stress can affect dimensional accuracy causing printed part dimensions to be out of specification. To produce high quality parts that have appropriate dimensional accuracy, it is important to have a procedure that can be implemented to reduce the residual stress that is accumulated during manufacturing. While it is easy to find papers that characterize and model the stress in LENS parts [2-4], little information can be found regarding techniques that are implemented to reduce the residual stress in the 3D printed parts. The aim of this research is to explore the effects of a heated print bed on the accumulation of residual stress in 3d printed parts made with LENS. This research is of particular interest to the aerospace and defense industries, and has the potential to impact many other markets as AM becomes a larger contributor in the worldwide approach to manufacturing.

1.2 Objective of Research

This Thesis will explore the feasibility of reducing the residual stress on 3d printed metal parts using LENS. The process of introducing additional heat into metal parts to reduce the residual stress during a manufacturing process is not new. Welders often raise the temperature of the parts that will be fused together to reduce stress in the welds [5-7]. If the stress in these welds is not reduced, warping and cracking of the system can occur. Adding heat to metal parts is not new in additive manufacturing research either. Various experiments have been performed on a powder bed selective laser sintering (SLS) systems [8, 9]. The uniqueness of this work is introduced by its application to the LENS printing platform. The traditional setup of most LENS systems produces thermal gradients of 400 K/mm or higher near the deposition zone [10, 11]. The high thermal gradients coupled with the raster patterns inherent to direct write AM systems causes rapid and localized heating and cooling of the part that can be as high as 500-600 K/s [10, 12]. High thermal gradients and rapid heating and cooling of LENS 3D printed metal parts can lead to unique mechanical properties [10, 13, 14]. It is believed that raising the temperature of the 3D printed metal part, will both reduce the thermal gradient, and decrease the

rapid heating and cooling which are both connected to the residual stress development [3, 10, 15]. The objective of this thesis is to determine if additional heating is a feasible approach to reducing the residual stress accumulation in 3D metal parts produced with Laser Engineered Net Shaping.

1.3 Methods of Research

This work evaluates the use of a pre-heated substrate and print bed to reduce residual stress in 3d printed metal part made with LENS. For this work samples were printed with the print bed set at varying temperatures. For each heated bed print, the LENS parts experience accumulation of residual stress. One of the ways that the residual stress manifests itself is through warping and distortion of the print substrate [16, 17]. By comparing the magnitude of distortion experienced at each of the bed temperatures, a comparison is made that determines the effect of print bed temperature on residual stress accumulation. A second set of experiments was performed that utilizes destructive residual stress measurement techniques. Digital Image Correlation (DIC) is used to measure the relaxation of stress after a section of the 3D printed part is removed. By comparing the magnitude of

deformation from parts printed at various platen temperatures, conclusions will be made about the impact of preheating on residual stress accumulation in the printed part. This thesis compares the results of each of these methods, and draws conclusions about residual stress reduction in 3d printed metal parts made on LENS.

1.4 Structure of Thesis

This thesis contains six chapters. Chapter one introduces the background, objective, and methods of research.

Chapter 2 is a survey of various manufacturing technologies for producing 3D metal parts. This review contains information on advantages and disadvantages of each process. A case is made to explain why it is important to reduce residual stress in 3D metal parts made with LENS printing technology.

Chapter 3 shows computational simulations that were performed to gain an understanding of the heating process, and its impact on the 3D metal part. This chapter compares the thermal gradients and maximum temperatures that can be expected at various print bed temperatures, and differing printed part orientations.

Chapter 4 describes the methods that were used in this research, and the experimental setup for each method. The techniques used to gather and record the data are also shown.

Chapter 5 documents the data that was collected during the experimentation using the methods described in this work. A comparison of the results of each method is also shown.

Chapter 6 summarizes the conclusions, future work, and impact of the research discussed in this thesis.

Chapter 2 Review of Metal Additive Manufacturing

2.1 Metal Additive Manufacturing

Additive manufacturing (AM) is an approach to make prototype and production parts to be produced in a layer wise fashion. The AM approach differs significantly from conventional manufacturing processes that 1) start with a billet of material and then cut away at the billet until the desired geometry is formed, or 2) require the use of expensive molds to form and shape a part as a molten material is poured into it. The ability to use AM to generate parts layer by layer, presents the opportunity to create structures with geometry that could not be developed using conventional methods. Recent software developments such as topology optimization rely on the use of AM capabilities to produce complex organic shaped structures. One of the many promising benefits of the more complex geometries from AM, is the capacity to transform multi-part assemblies into a single part that provides the same function as the original assembly [18]. Since the overarching goal of this paper is to reduce the residual stress in 3D printed metal parts, the remainder of this chapter will describe the key processes used to make AM metal parts from powdered metal.

2.2 Binder Jetting

Binder Jet printing is a type of powder bed printing that utilizes a glue or “binder” to adhere the particles together. In binder jet printing, the process starts off with a solid model of the printable object. This model is processed into code that tells the printer layer by layer where the binder should be deposited. For the binder jet process, a substrate is coated with a thin layer of powder. An inkjet head then dispenses the liquid binding material in a pattern that represents a horizontal slice of the first layer of the part. Then another thin layer of powder is spread over the part, and the binder is dispersed in a pattern representative of the second slice of the 3D part. This process repeats until all subsequent layers of the 3D printed part are deposited. Once all layers are deposited, the part is removed and must be post processed to remove the binder and sinter the powder particles. A representative image of the binder jet printing process is shown in Figure 1.

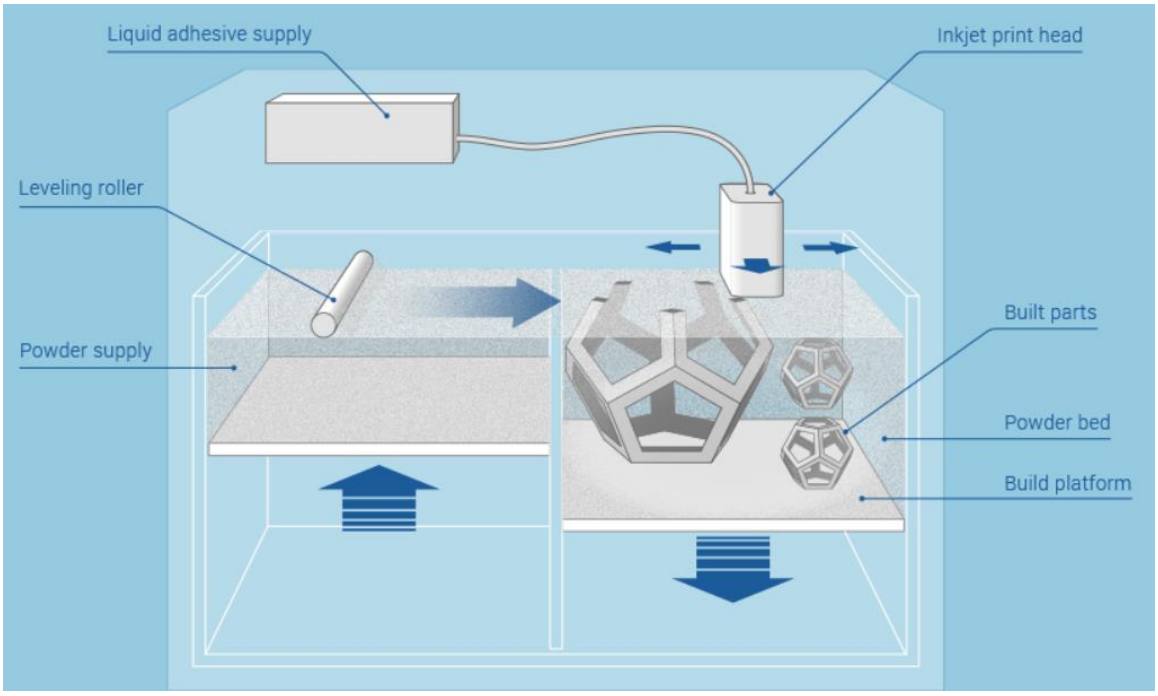

Figure 1 Schematic of binder jet printer [19]

There are many advantages of using binder jetting to print metal. Binder jet printers are less expensive than other forms of metal printing especially when compared to those that use a laser [17, 19]. Because this style of printers uses an ink jet to deposit the binder, it can print small features and has great dimensional accuracy. Both feature size and dimensional accuracy are limited by the size of powder that is used for the printing [17, 19, 20]. Since the binder jet method of printing metal parts does not include localized heating of particles to induce melting, parts can be created that have very little residual stress [17, 21]. The main deficiency of binder jet printing is that because of its

inability to fully densify the printed powder, it cannot be directly applied to many practical engineering applications [17, 20-22]. Studies suggest that binder jet printing has ability to achieve a maximum of 50-60% theoretical density in metals [20, 21]. Densities in this range are not acceptable for most applications outside of prototyping. In most cases, post processing is required to achieve acceptable 3D printed parts.

2.3 Powder Bed Fusion

Selective laser sintering (SLS) and electron beam powder bed (EBPB) are another form of powder bed printing. Selective Laser sintering uses a laser to melt the powdered metal, and electron beam powder bed uses and electron beam to melt the metal. SLS and EBPB printers use the same process of converting a CAD solid model into code that represents the desired part geometry sliced into multiple layers. Instead of the code telling the printer where to deposit a binder (like in binder jet), the code used in a SLS or EBPB printer tells the printer where to focus and raster the laser or electron beam. As the beam focus is moved around on the layer of powder, it melts the powder causing the metal powder particles to fuse together. As the layers of powder are fused together,

a 3D metal part is produced. Figure 2 shows a schematic of a typical SLS or EBPB system.

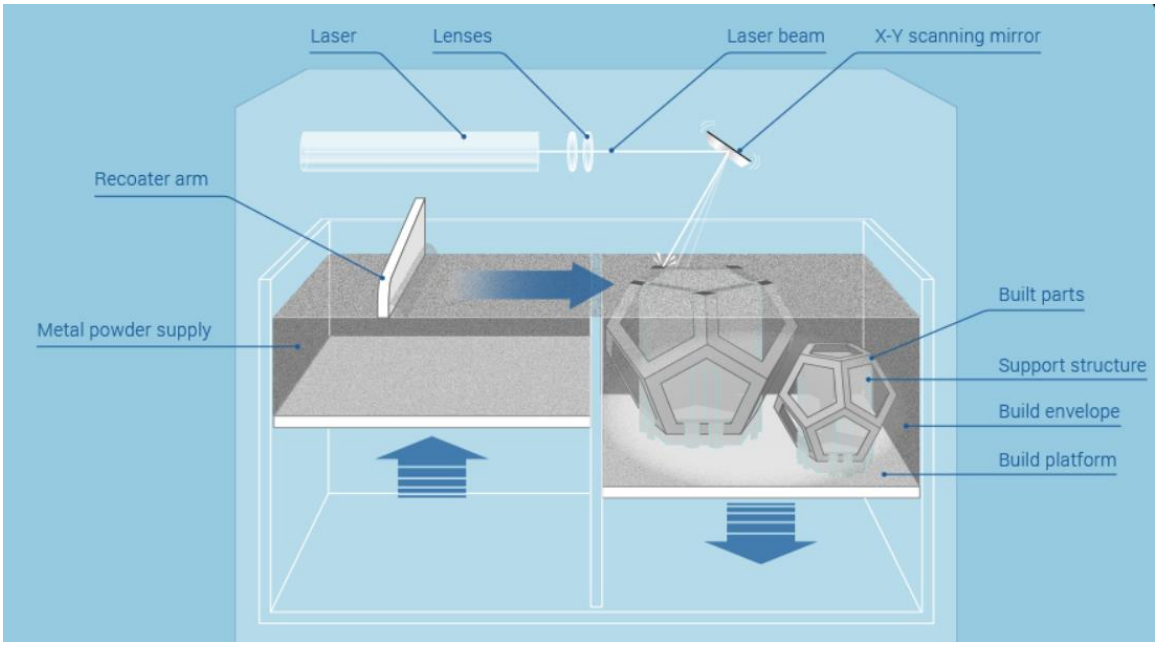

Figure 2 Schematic of SLS printer [23]

The advantage of fusion style powder bed printers over the binder jet style is that powder particles are melted during the print. The particle fusion that is achieved eliminates many of the post processing steps necessary to achieve fully dense parts, as in the binder jet process. Other advantages characteristic of SLS and EBPB systems are the ability to produce high resolution features, internal passages, and maintain dimensional control [17, 24]. SLS and EBPB printers have the capability of producing parts that are 95-99+% theoretical density which contributes great mechanical properties that are achieved [17, 24]. Metal parts that are

produced on SLS and EBPB printers can have large amounts of residual stress because of the localized heating and cooling resulting from the laser and electron beams melting the powder [8, 9, 17, 22].

2.4 Laser Engineered Net Shaping

The Laser Engineered Net Shaping (LENS®) process uses a focused laser beam and fluidized powder streams to deposit material onto a substrate (Figure 3). Multiple powder streams are oriented to converge to a point coincident with the focus plane of high powered laser. The laser melts the substrate surface and the powder is consumed in the melt pool to increase the volume and affect the deposition. By rastering the combined laser/powder streams relative to the substrate surface, features can be printed.

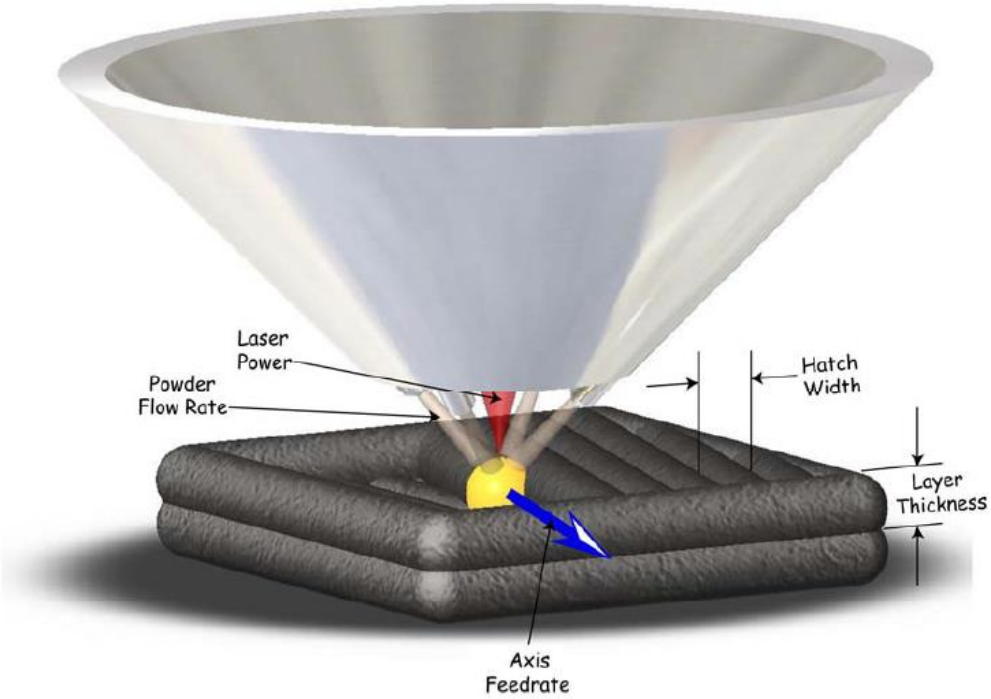

Figure 3 Schematic of LENS print head [25]

LENS, like the other processes discussed in this thesis allows users to 3D print mechanical components directly from a computer aided design (CAD) solid model. To print 3D objects, a toolpath is created (manually or from a CAD solid model) to direct the deposition process and add material where it is needed on a layer by layer basis (Figure 4).

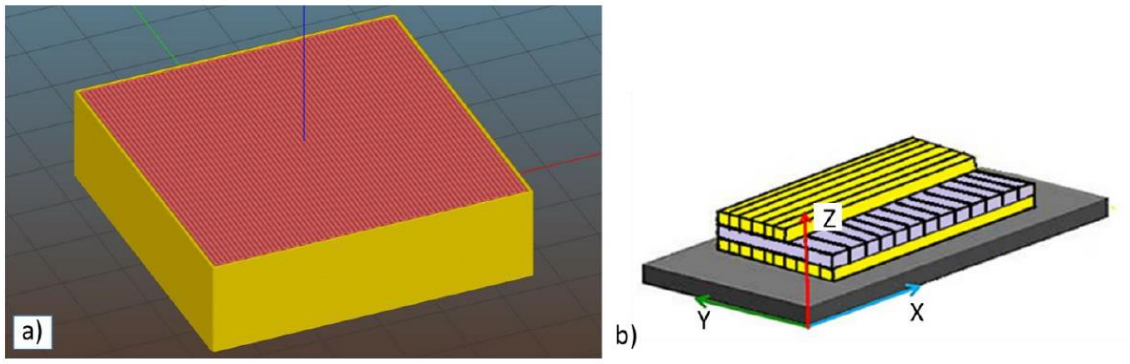

Figure 4 a) Slic3r software used to convert STL into a LENS toolpath b) example of cross-hatching of layers that was used in this work. [26]

The LENS process can produce parts from a variety of different metals such as steel, stainless steel, nickel, copper, nickel based alloys, and titanium [3]. Because this style printer is a powder fed system rather than a powder bed system, it has the capability of creating parts that are composed of more than one type of material. LENS can also produce parts that are functionally graded from one material to the next. This gives a designer the ability to utilize material properties of one material in a certain section of the part, and completely different properties of a different material in an adjacent section [17, 27]. Another unique capability of LENS is that it can be used to repair warn or damaged components [25]. LENS has been certified by Rolls Royce, and the U.S. Army as an acceptable form of repair for over 20 different components [17]. Some of these components include parts for a turbine engine, and lift fan blisk parts on a joint fighter aircraft. Even though LENS has distinct advantages over many of the other common additive

manufacturing tools, there are also disadvantages to this process as well. Much like the sintering powder bed style printers, the localized heating, cooling, and rastering back and forth causes residual stress to accumulate in the 3D printed part [2, 3, 11, 19, 28, 29]. Residual stresses inherent to 3D printed parts from LENS can be large enough to warp and distort the parts. The unique capabilities of LENS make it desirable to many industries including aerospace and defense. The driving force behind this research is to lessen the negative characteristic of LENS, high residual stress, to be able to take greater advantage of unique capabilities this technology possesses.

Chapter 3 Thermal Analysis

This thesis considers the use of a heated print bed to reduce residual stress in 3D printed parts made using a LENS 3D printer. This work will focus on the use of 304L stainless-steel. The feasibility of this work is dependent on the magnitude of heating that must be achieved to reduce residual stress in stainless steel. The goal of this work is to demonstrate that the necessary level of preheating can be achieved to reduce stress in 3D printed LENS parts. In an article published by the British Stainless-Steel Association (BSSA), there is a table of treatments that can be used as guidelines for relieving stress in stainless steel parts [30]. All the prescribed treatments, except for one, require prolonged temperatures more than 900℃. While these procedures may be best for many applications, temperatures of such a high magnitude can be detrimental to a 3D printer with precision motion stages and fragile optics system such as LENS. The heat treatment chart provided in the BSSA article does include one heat treatment that recommends much lower temperature. This treatment is described as a dimensional stability process, and only requires a temperature of 475℃ with a slow cool of approximately 4 hours for every 25mm of section. This process relieves enough of the stress, that a

part would be dimensionally stable which in many cases is all that is needed for high quality LENS 3D printed parts. If the temperature of the platen were set to 475℃ then allowed to cool down slowly, according to the BSSA procedure it is conceivable that much of the stress would be relieved. The reason that they suggest 475℃ is that it is below the temperature at which stainless steel is at risk for being sensitized. Figure 5 is a TTT diagram for 304 Stainless steel, and the curves on this diagram show the regions at which stainless steel is at risk for sensitizing [31]. In these regions of the plot, the conditions are correct so that coarse chromium carbide particles form at the grain boundaries causing the stainless steel to become much more brittle. Sensitizing also causes the stainless steel to be susceptible to corrosion. It is also important to note how the time to sensitize changes as the carbon content in the stainless-steel changes. For this study we are using 304L SS which is a low carbon version of 304. 304L contains 0.03% or less carbon which reduces the temperature ranges at which sensitizing occurs, and pushes the time out to almost 10 hours for the chromium carbide particles to form. As the carbon content goes up, the time to form the chromium carbide goes down to minutes. To reduce the residual stress in stainless steel it is important to take the temperature as high as

possible while also staying out of the regions in Figure 5 304L Stainless Steel TTT diagram [31]. That is why almost all heat treatments recommend temperatures above 900℃ or below 475℃. For the setup that we have on our LENS printer it is not possible to reach temperatures of 900℃, so we will show temperatures below that range.

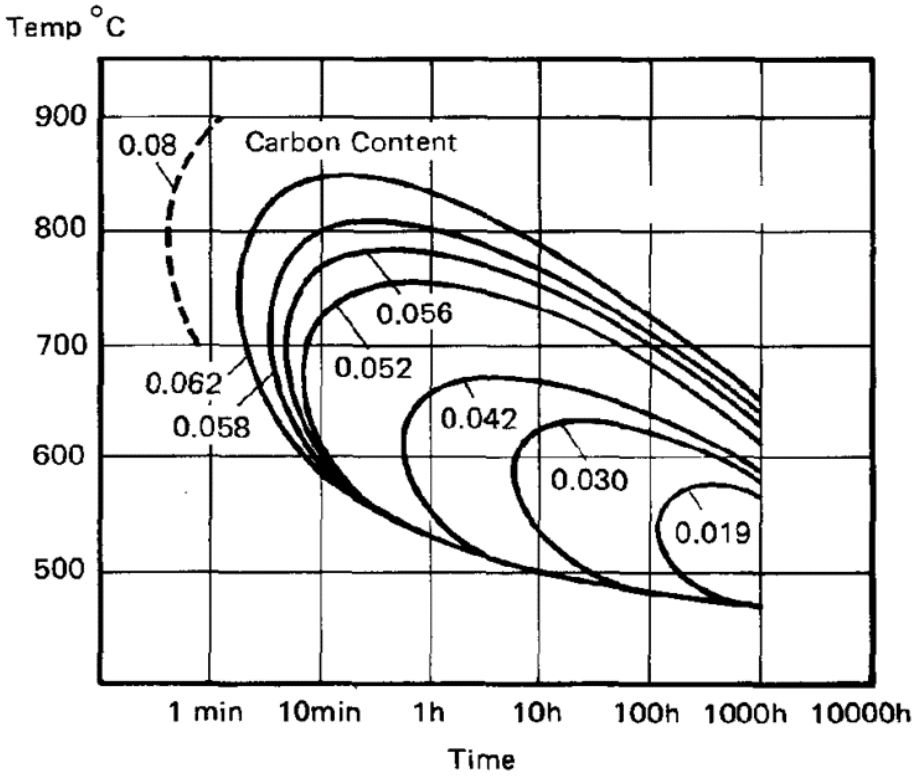

Figure 5 304L Stainless Steel TTT diagram [31]

This chapter will focus on understanding how geometric and thermal conditions change the heat transfer from the heated platen into the 3D printed part. This chapter will also develop an understanding of how these geometric and thermal variables change the thermal gradient through the height of the 3D part. It is believed that as the thermal gradient is minimized, and the maximum temperature is increased, that the stress accumulation in a metal 3D printed part will be reduced.

3.1 Substrate Warping

Residual stress buildup is common in all types of 3D printing. In metal 3D printed parts, it is common for the stress buildup in the part to be so strong that the 3D metal part will warp. One additional way that the residual stress manifests itself in the form of a warped substrate. Since substrate heating is the method being investigated to reduce residual stress in 3D printed parts, it is necessary to comprehend how warping affects the heat transferred to the 3D printed part. To understand how substrate warping was affecting substrate temperature during the printing process, a thermal simulation was created in SolidWorks®. For this simulation, the temperature of the t-slot platen was set to 450℃, the ambient

temperature of the argon surrounding the part was 35℃. SolidWorks has a library of materials containing thermal and material properties for various materials. From this library the platen was assigned properties for 6061 Aluminum, and the substrate was assigned properties for 304 stainless steel. The convection of the heated parts to the surrounding the parts is modeled by assigning a thermal conductivity of the gas surrounding the parts. The LENS 3D parts are printed in an argon environment, and since the thermal conductivity of argon changes with temperature, the thermal conductivity of the Argon environment was determined by interpolating the data given by in Figure 6.

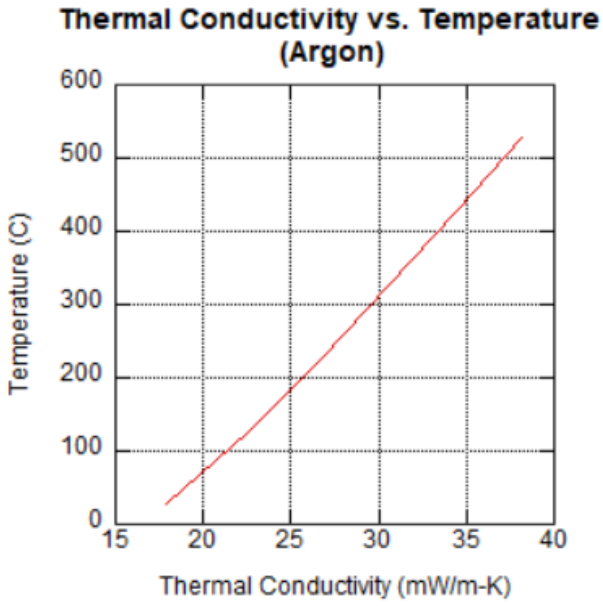

Figure 6 Thermal conductivity vs temperature for argon [32]

It is typical that during a LENS 3D print, a substrate can be warped from flat within 0.002” to having over 0.25” of curl on all sides. Simulations were performed using the 450°C platen temperature for a flat substrate and a warped substrate. After a 3D printed metal part has been built, the substrate is curled in the Z-axis direction all around the part. The farther away the position on the substrate is from the 3D printed part, the greater the displacement from the platen. If the 3D printed part was manufactured in the center of the substrate, the corners and edges of the substrate will have the greatest displacement relative from the surface of the platen. The profile of a typically shaped warped substrate is shown in Figure 7. The results from these simulations show that when the substrate stays in contact with the platen (Figure 8a), the substrate temperature is very close to that of the platen. However, as the substrate warps and loses contact with the platen, the thermal conductivity of stainless steel is not sufficient to maintain a uniform substrate temperature, causing large thermal gradients across the substrate. The temperature variation can be hundreds of degrees across the substrate, which is not a desirable research condition (Figure 8b).

Figure 7 Side view of substrate on platen. a) Represents typical substrate prior to print with no warping. b) Represents typical warping of substrate experienced during a LENS 3D print. Platen in red and substrate in blue.

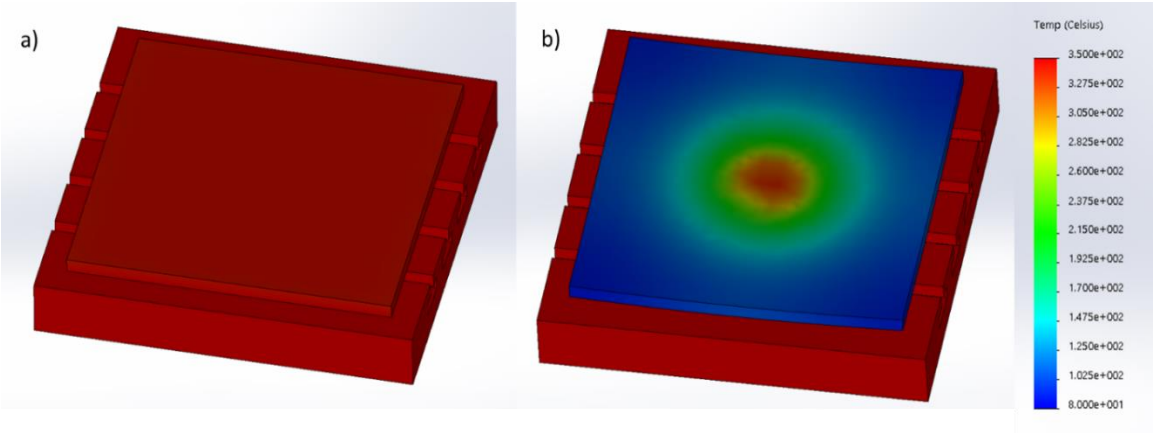

Figure 8 Temperature of flat substrate vs warped substrate. Temperature simulation that was produced in SolidWorks of substrate sitting on a platen at 450 ℃. a) Flat substrate b) Substrate that has warped due to residual stress.

The simulation results strongly suggest that maintaining intimate contact between the substrate and heated platen is essential for good heat transfer into the 3D printed part. Since conducting heat into the 3D printed part is the primary goal of heating the substrate, it is obvious that something needs to be done to keep the substrate from warping. If heat can be conducted efficiently into the part by maintaining a

planar substrate, then results from an experiment on using temperature to relieve residual stress will be much more accurate. For this reason, it is necessary for a method to be developed that ensures that the platen and substrate remain in contact with each other throughout the entire 3D print process.

3.2 Transient to Steady State Analysis

The use of a heated substrate is the method being investigated to relieve the stress in a 3D printed part. The temperature on the print current printer setup is measured from the heated print bed not from the substrate itself (this setup will be shown in chapter 4). Since the desire is to know the temperature of the substrate, not the print bed, it is important to know what the temperature of the substrate in relationship to the platen. The simulation shown in Figure 9 was designed to demonstrate what the difference in temperature is between actual substrate temperature versus platen temperature. The simulation was set up as a transient study where the temperature of the platen and the substrate both start off at 25℃. A heating of 1200W is then applied to the platen which represents the heat coming from the cartridge heaters. A probe was set up in the simulation to regulate the

temperature of the platen between 445℃ and 455℃ just as a PID controller would do in the LENS 3D printer. The simulation was set to calculate the temperature over the course of 2 hours. After the simulation was ran, the data was collected and plotted for the temperature of the platen (taken at the location of the thermocouple) and the surface of the substrate. Thermocouple data is shown in Figure 10.

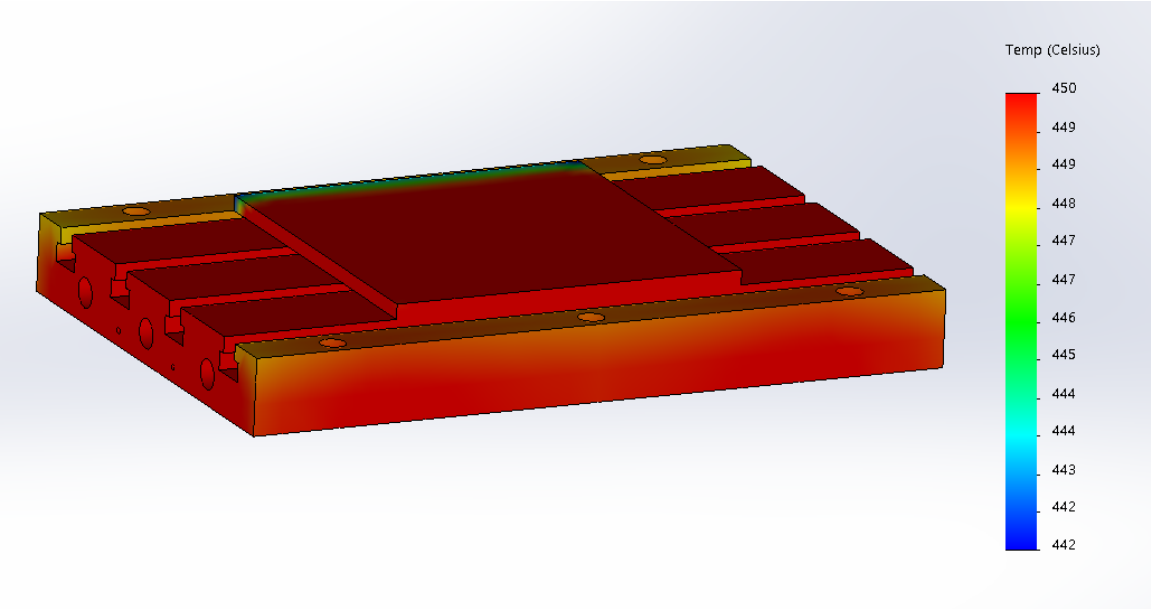

Figure 9 Substrate and platen at the end of time study simulation.

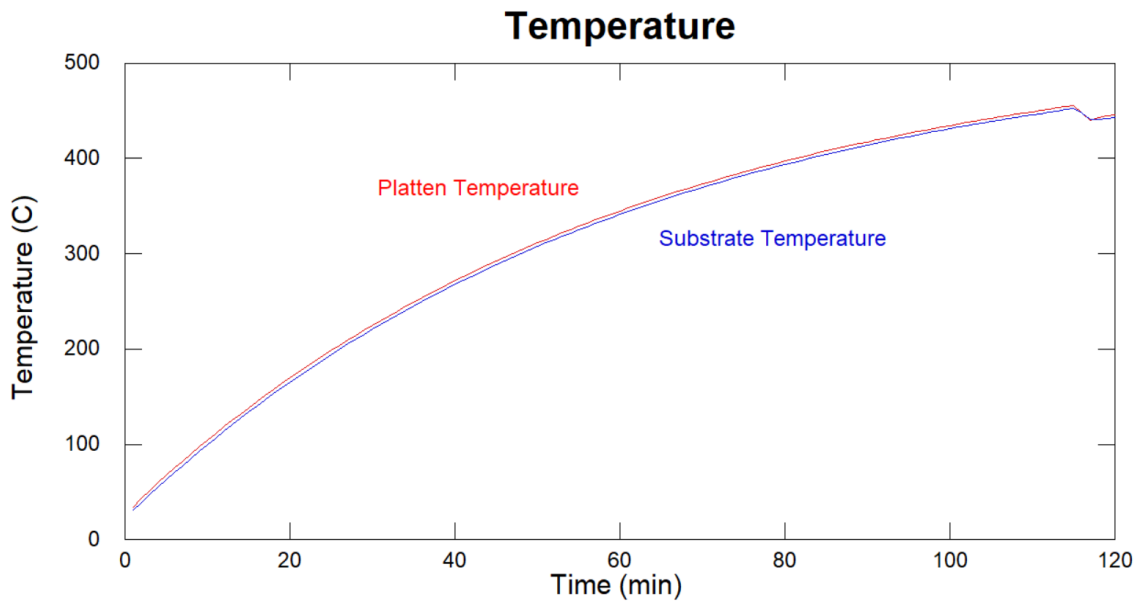

Figure 10 Graph of the temperature of the substrate and platen separately during warmup procedure simulation.

The data gathered from simulating the platen and substrate through a warmup cycle shows at least two pieces of information that are important. First, there is very little time delay from when the platen reaches a temperature of 450℃ and when the substrate reaches its maximum temperature. This is important because if there were a time delay of 10 minutes then it would be desirable to start the 3D printing process 10 minutes after the platen reaches its set temperature. However, since there is very little if any time delay the printing process can be started as soon as the platen achieves the set temperature. Second, the difference between the platen and substrate temperatures is essentially constant throughout the process. For this simulation, the difference in

temperatures was about 5 degrees. This means if 450℃ is desired as the substrate temperature, the platen would need to be set to 455℃.

3.3 Thermal Gradient

Now that a method has been developed to ensure the substrate is at the proper temperature, the simulation from Figure 8a and graph from Figure 10 show that it can safely be assumed that at steady state the substrate is very close to the same temperature as the platen. Studying the substrate temp is important since the substrate provides a conduit to heating of the 3D printed part. It is not expected that the 3D printed part will maintain a constant temperature especially as its build layers get farther and farther away from the substrate. It is important that we understand the thermal gradient over the height of a 3D part, and how the thermal gradient changes in different environments. The thermal gradient created during the manufacturing process of 3D printed metal parts is believed to be a large contributor to stress buildup [3]. To avert stress building up it is important to maintain a low thermal gradient during the 3D printing process. To learn more about this thermal gradient in the 3D printed parts, the next questions that need to be addressed are: (1) what is the

thermal gradient across the vertical height of the part and (2) does temperature of the platen affect this gradient? To answer these questions another simulation was designed in SolidWorks. This simulation includes the same platen and substrate from the previous simulations, however in the new simulation a 3D printed part is included, and is representative of the 3D part described in method 1 of chapter 4. For this simulation three different values for the platen temperature will be shown with a constant heat power input that represents the thermal energy that would be added to the 3D printed part through the laser. SolidWorks does not allow the modeling of the laser input directly so instead an input that approximated a full layer heating that is observed during a typical process. This number was determined by taking the spectral absorptivity of the stainless-steel multiplying it by the power output of the laser. For the simulations shown in this chapter, a laser input of 400W was used and spectral absorptivity of 30% leaving a thermal input of 120W into the top surface of the 3D part [33, 34]. Figure 11 shows the simulation without platen heating, in Figure 12 the platen is $250°C$, and in Figure 13 the platen is set to $450°C$. Figure 11-Figure 13 are marked with the temperature that is expected at the top and bottom of the 3D printed part which are represented by node 630 and 354 respectively. The temperature

reading at these nodes are used to find the temperature gradient from top to bottom of the 3D printed part.

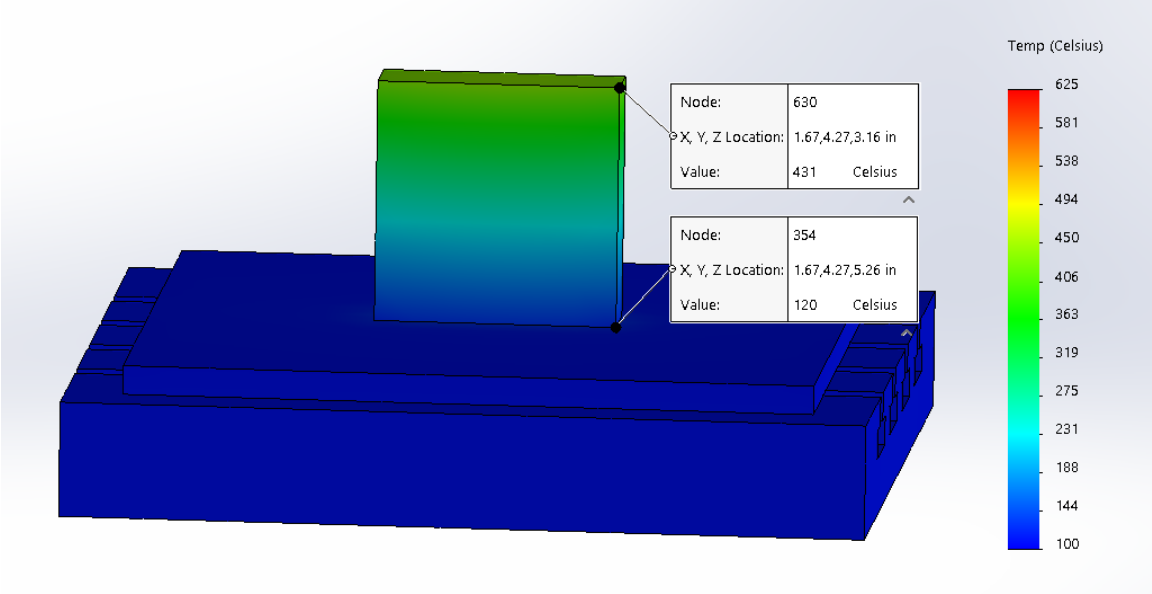

Figure 11 Temperature gradient of part with no added heat through platen.

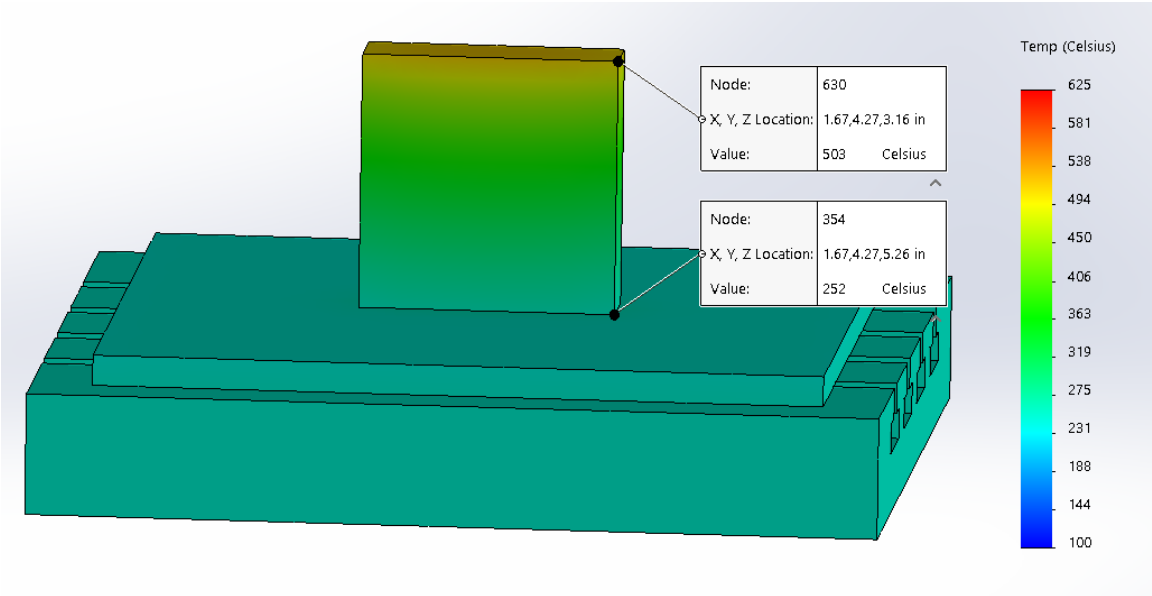

Figure 12 Temperature gradient of part with 250℃ platen.

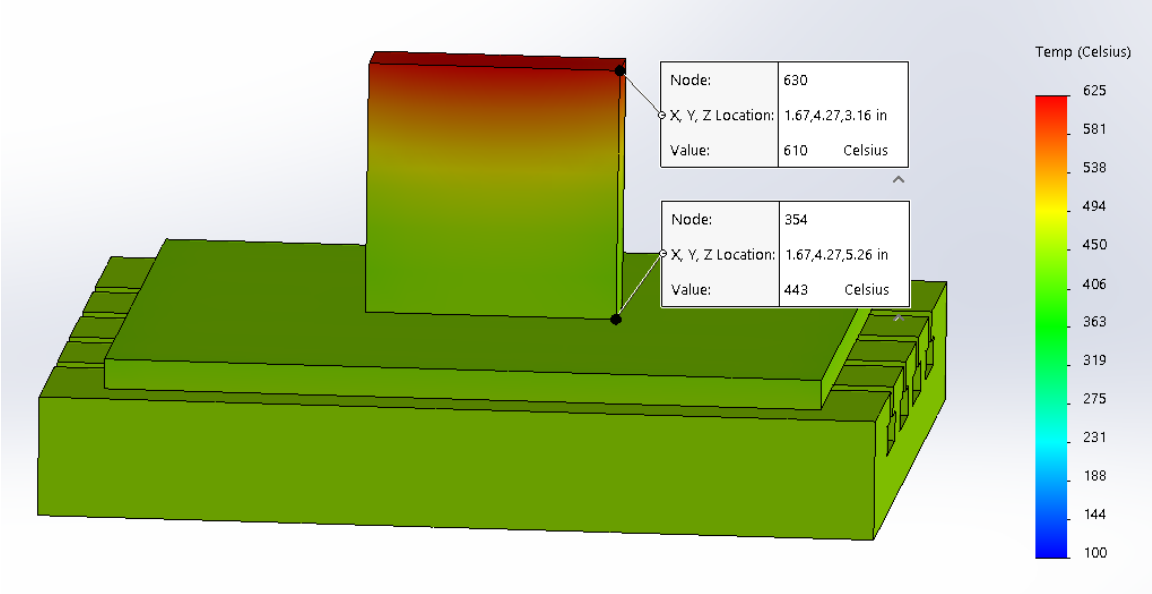

Figure 13 Temperature gradient part with 450℃ platen

When there is no heat added through the platen, shown in Figure 11, the top of the 3D printed part is 431℃ and the bottom is 120℃. This means that the temperature gradient over the height of the 3D printed part is 311℃. If the platen temperature is set to 250℃ as shown in Figure 12, the top of the 3D printed part increases to 503℃ and the bottom moves to 252℃. In this situation, the temperature gradient over the height of the 3D printed part decreases to 251℃. For the last simulation, the platen was set to 450℃ and is shown in Figure 13. For this simulation, the top of the 3D printed part increases to 610℃ and the bottom of the same part increases to 443℃ which decreases the thermal gradient over the height of the 3D printed part down to 167℃. This data demonstrates

that as the platen temperature is increased, the thermal gradient is decreased. When the thermal gradient is decreased, the residual stress should be decreased. It is also important to note that as the print bed temperature increases, the temperature of the top of the part also increases. The higher temperature of the top of the part is likely to provide a better condition for stress relief, therefore preheating is being considered as a method to reduce residual stress.

3.4 Printed Part Orientation

It has now been shown what the approximate thermal gradient from the bottom to the top of a 3D printed part is expected to be at different platen temperatures. While this information is important and can help the informed user design experiments to test this information, a couple of important questions are left unanswered. One of the benefits of additive manufacturing is that parts can be printed in multiple different orientations on the substrate. Since many 3D printed parts can have different mechanical properties in the Z direction than they do in the X-Y direction this allows the user to orient the part in such a way as these anisotropic properties can be used to the designers' advantage. The question then arises as to how changing the orientation of the 3D printed

part affects the thermal gradient and therefore the stress relief in that part? To study this concept another set of SolidWorks simulations was created. For both simulations, the platen was set to 450℃ and the laser power was once again represented by a heat input on the top surface of the 3D printed part. For this study, two different orientations of the part were used. The first orientation is shown in Figure 14 and represents the 3D printed part being manufactured on its side so that the geometry of the part is as close to the substrate as possible. This orientation makes the vertical height of the part in the Z- axis direction as small as possible with this predetermined 3D part geometry. The second orientation, shown in Figure 15, is the same as the previous thermal gradient simulations and represents the part oriented in such a way as to make the Z- axis height of the part as large as possible. These simulations show how the thermal gradient changes as the orientation of the 3D printed part is changed.

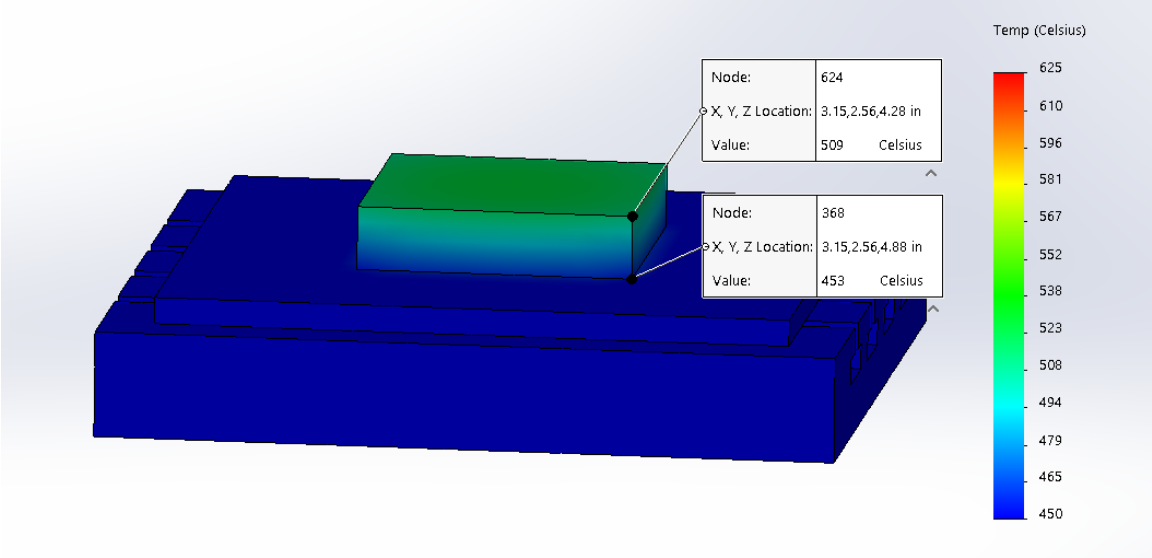

Figure 14 Temperature gradient on horizontally oriented part with 450°C platen

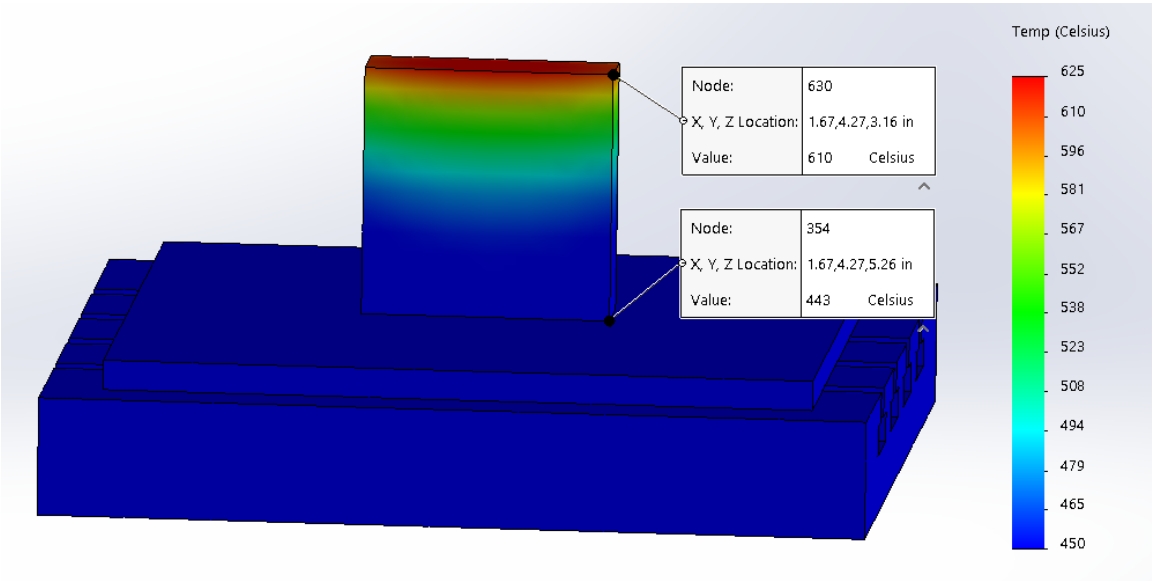

Figure 15 Temperature gradient on vertically oriented part with 450°C platen

When the 3D printed part is oriented as shown in Figure 14, the top of the part is simulated to be at 509℃ and the bottom of the part is at 453℃. This orientation produces a thermal gradient of 53℃. When the 3D printed part is oriented in the

vertical direction as shown in Figure 15, the top of the part is at a temperature of 610℃ and the bottom near the substrate the temperature is simulated to be 443℃. This means with a vertical orientation of the 3D printed part there is a thermal gradient of 167℃. Two important things come from this simulation. First, when the 3D printed part is oriented horizontally as shown in Figure 14 the thermal gradient is much lower than that of the vertically oriented part in Figure 15. Second, the maximum temperature of the 3D printed part is over 100℃ higher when the part is oriented vertically. As has been discussed in earlier sections of this paper, it is known that the thermal gradient plays a role in how much stress is developed in a 3D part as it is printed [3]. It is also important to remember that the maximum temperature that a stainless-steel part acquires plays an important role in how much stress is relieved. As the temperature near the melt pool is increased, the quench rate of the molten metal is decreased allowing reducing the stress accumulation from this source. For the case of relieving stress in 3D printed parts it is desirable to have both a low thermal gradient and high temperature near the melt pool. The data from these two simulations suggests that the different part orientations could result in differing modes of stress reductions. The horizontally oriented part reduces stress through a reduced

thermal gradient, and the vertically oriented part reduces stress through increased temperature near the melt pool.

Analysis of the thermal gradient on the 3D printed parts discussed in this section is complicated, and it is unclear if the difference between minimum and maximum temperature is the best way to approach this problem. Another way of looking at the thermal gradient is to look at the temperature change per inch through the height of the 3D part. To consider the thermal gradient per inch on the horizontal 3D part, the temperature change over the height of the 3D part, 53 ℃, is divided by the 0.6" height of the part. This calculation produces a thermal gradient of 88.33℃ per inch. However, when this same calculate is performed for the vertical orientation, the same calculation shows that a 167℃ thermal difference over the height of a 2.1-inch 3D part gives a thermal gradient of 79.52℃ per inch. These calculations of thermal gradient per inch are relatively close to each other, but would lead the user of the information to believe that less stress would be developed in the 3D part with the vertical orientation. This thesis will not investigate how part orientation changes the residual stress, however it is expected that part orientation would have an impact even if the platen

temperature were the same during the manufacturing of a part at both orientations.

Chapter 4 Experimental Setup

To study the effects of print bed preheating on residual stress, two methods of gathering data have been developed. The first method measures the amount of distortion introduced into the substrate to measure the residual stress. The second method of measuring stress determines the amount of stress that relaxes when a portion of the 3D printed part is removed. For both techniques, metal parts are printed at various print bed temperatures. The substrate warping method represents a feasibility study that offers the ability to quickly produce results. Measuring the deformation of a substrate gives qualitative information on the amount residual stress that is accumulated in a 3D printed metal part during print. The slitting method is more consistent with methods found in literature, and offers advantages over measuring substrate deformation. First, the slitting method measures deformation in the actual printed part instead of the substrate. Second, measurements acquired by this method can be used to solve for quantitative data about the stress in the 3D metal part. This chapter will describe each method in further detail, and

explain how residual stress data is extracted using each approach.

4.1 Method 1 - Substrate Warping Method

The substrate warping method takes advantage of the fact that residual stress in a 3D printed metal part manifests itself in the warping of the substrate it was printed on. This method does not provide detailed knowledge of placement or direction of stress in the part, but can provide the user with a quick idea of the magnitude of the stress. The substrates used in these experiments were 6″ x 6″ x ¼″ flat ground 304 substrates purchased from McMaster-Carr. The flatness of the substrate was measured before and after 3D printing onto the substrate. Measurements were taken on each plate at the locations shown in Figure 16. These measurements were made at the same location on all substrates both before and after the deposition. A total of 8 measurements were made for each substrate. These locations were selected to avoid the 3D printed part that would be printed in the center of the substrate. To minimize measuring errors associated with burrs or other edge defect, it was decided to have all 8 of the measurement points 0.25 inches away from the edge of the substrate. A measurement was taken in each corner of the

substrate, and at a point half way in between each corner (Figure 16).

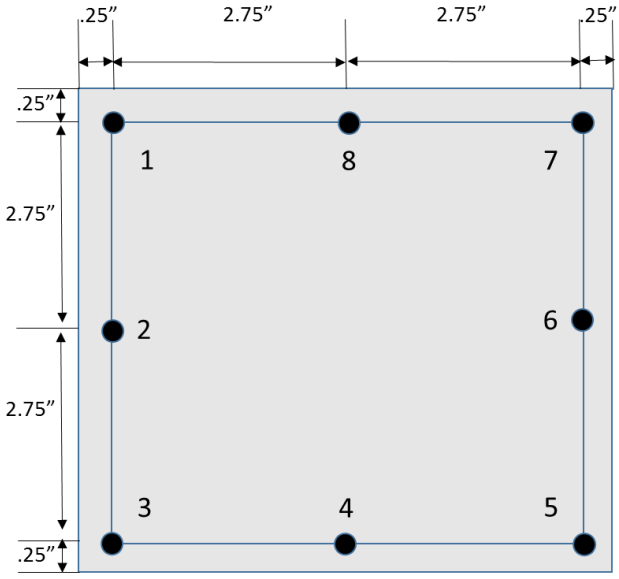

Figure 16 Diagram that shows the position of the 8 measurement locations that were used to measure the flatness of the substrate both before and after the part was made.

As previously discussed, the substrates used in this study were 304 stainless steel, and had been precision ground parallel with a specified manufacturing tolerance of ± 0.002 inches. To verify the flatness of the substrates before the part was printed on to the substrate a digital indicator (Figure 17) was used to take measurements in the 8 predetermined locations of the substrate. The first digital indicator used in this experiment was made by Mahr Federal, and is accurate to ± 0.00005 inches. In this setup, both the substrate and the indicator were positioned on a precision ground granite slab to minimize any error that could be

introduced from an uneven measuring surface. After all the parts were manufactured it was discovered that many of the substrates had warped enough that the first indicator, which was used for the initial measurements, did not have enough range of travel to do the post deposition measurements. It was also difficult to prevent the warped substrates from rocking on the flat surface. These problems were solved by using a different setup for the warped substrate measurements. This setup consisted of a triple ball bearing platform that stabilized the substrate without allowing it to rock on the warped surface, and a dial indicator with a large enough range of motion to account for the large distortion in the warped substrate (Figure 18). The second dial indicator used in the post manufacturing measurements was made by Starrett, and has an accuracy of ± 0.0005 inches. All substrate measurements, both warped and flat, used measuring point 1 as the zero-reference point and all other recorded numbers represent a variation from the zero-reference point.

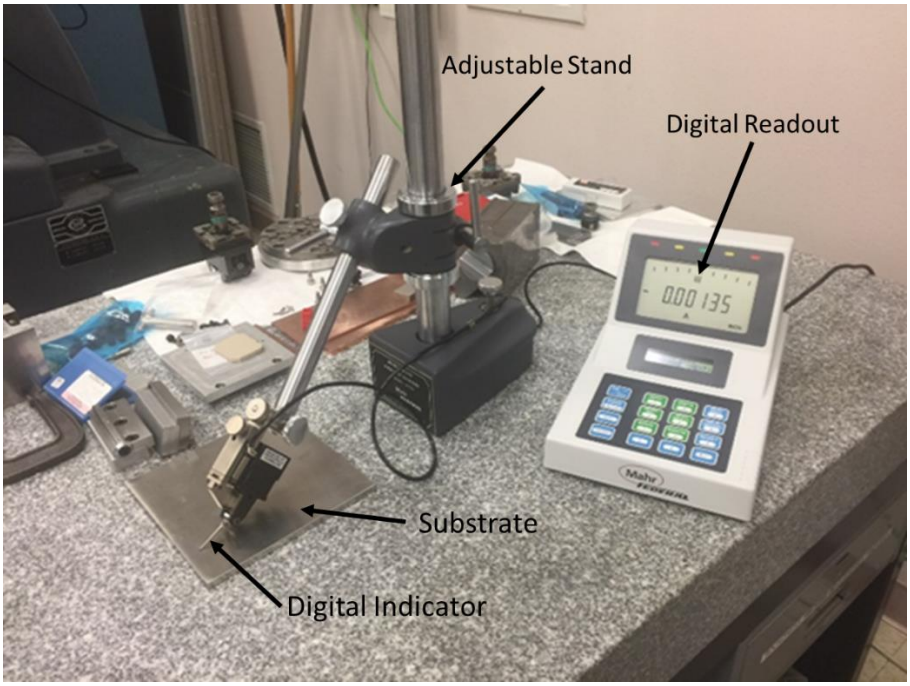

Figure 17 Flatness measurement setup for substrate prior to LENS build using a digital indicator. Measurements are taken on a leveled and precision ground granite slab to ensure accuracy.

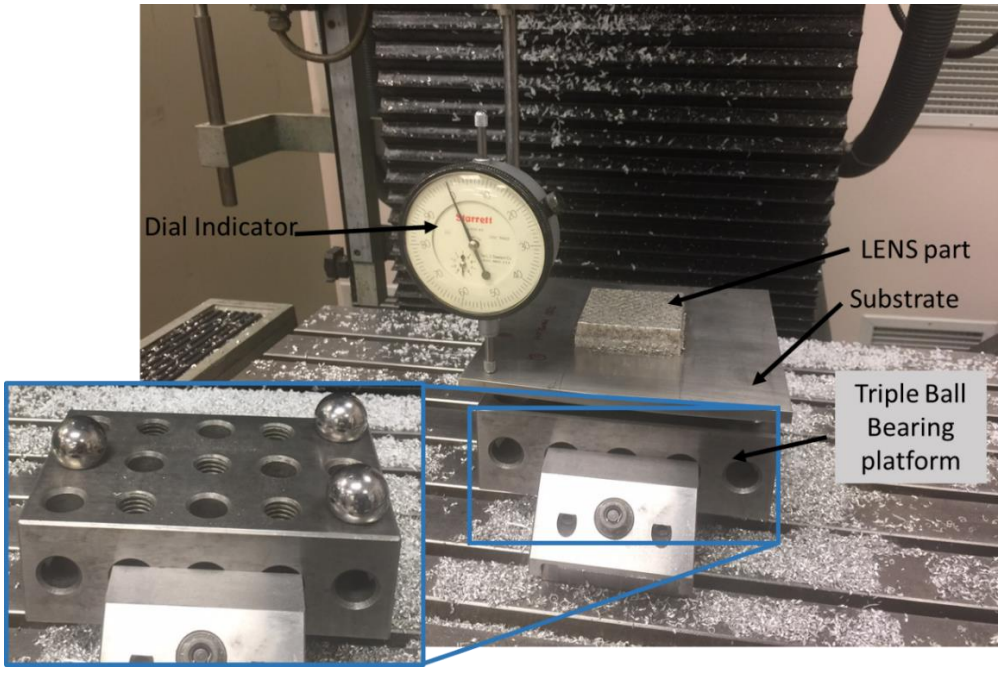

Figure 18 Flatness measurement setup for after part build using a dial indicator. Substrate is held on a triple ball bearing platform to provide stability on the warped substrate.

The part geometry chosen for this study was selected to allow the 3D printed samples to be used in other tests after distortion measurements were made (not discussed in this thesis). The 3D printed part designed so that after measuring distortion, residual stress measurements will be made using a holographic technique and then the 2.1 in x 2.1 in x 0.6 blocks will be machined into 9 different test specimens for mechanical testing of the samples. As shown in Figure 19. the block contains 8 tension specimens, and 1 compact tension specimen. This holographic stress measurement technique determines the bulk stress within the 3D printed part and can be used to determine what portion of the stress build up is close to the substrate, or close to the top surface of the block that was manufactured. Results from the holographic test specimens will not be discussed in this work. These testing blocks were built at 4 different substrate temperatures, no substrate heat input, 150°C, 250°C, and 350°C so comparisons could be made on how substrate temperature affects the residual stress.

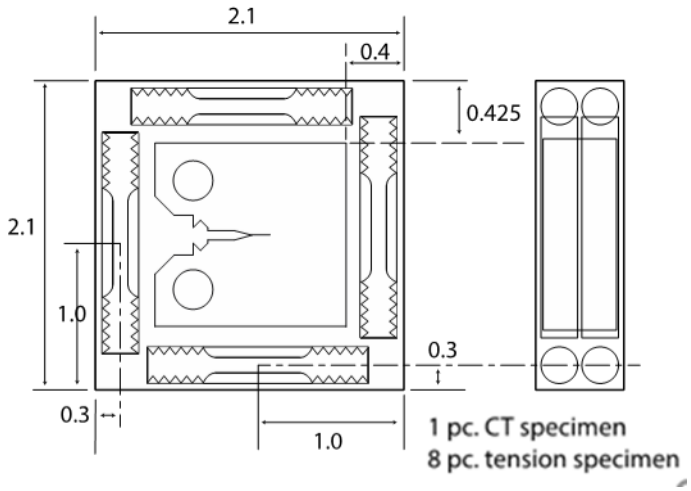

Figure 19 Drawing of test specimen that are designed to be machined out of the LENS part that was made in these experiments. The 2.1" x 2.1" x .6" block is designed to have 8 tensile specimens, and 1 compact tension specimen.

Table 1 LENS processing parameters for substrate warping method

Laser Power	500 [W]
Powder Feedrate	6.5[g/min]
Layer Thickness	0.25 [mm]
Hatch Spacing	0.8 [mm]
Parameter Deposition Speed	450 [mm/min]
Infill Deposition Speed	600 [mm/min]

The clamping configuration shown in Figure 20a was used in the experiments where substrate heating temperature was varied from approximately 35°C to 350°C. This first clamping configuration that consists of two clamps placed on opposite sides of the substrate. The two clamps were placed away from the corners, allowing them the freedom to distort from stress. Because of the information learned from the simulations in chapter 3 it was decided to try a second clamping configuration. The second clamping configuration utilized

six clamps, adding one clamp to each corner of the substrate (Figure 20b). Having a clamp in each corner of the substrate, constrains the substrate and makes it more difficult for the substrate to warp. This second clamping method also helps the substrate remain in contact with the platen.

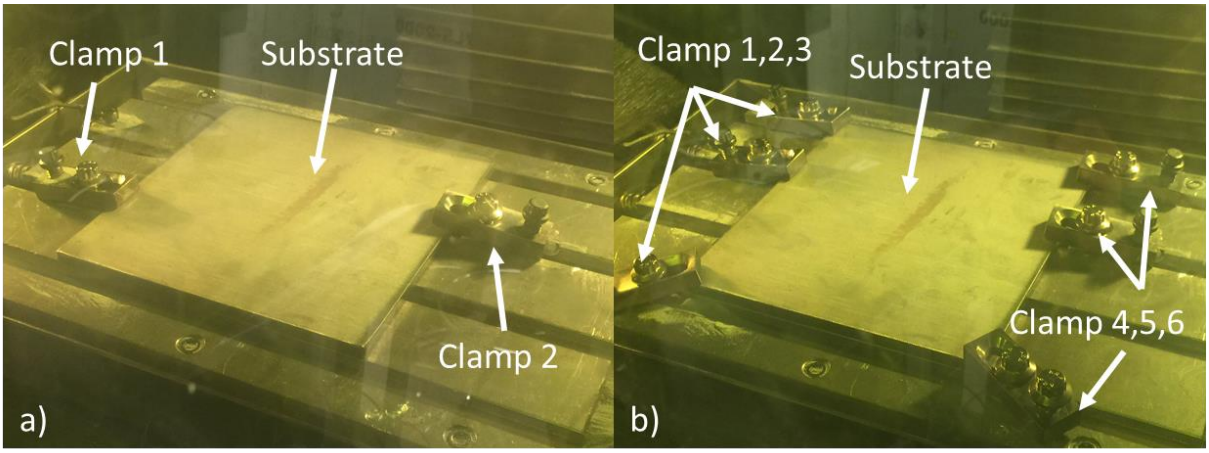

Figure 20 Substrate clamping methods a) clamped in two places allowing the substrate to move more freely b) clamped in six places holding the substrate onto the heated platen allowing for more heat transfer into the substrate.

4.2 Method 2 – The Slitting Method

There are two different classes of residual stress measurements that are commonly used in literature. These two classes can be categorized as destructive, and non-destructive. The advantage of using the non-destructive class of residual stress measurements is that the part is preserved. However, non-destructive methods take large amounts of time to calibrate for part geometry and material [35]. These characteristics makes the non-destructive methods perfect for

quality control applications but are more difficult to use in settings where low numbers of parts are analyzed between calibrations. In comparison, destructive methods require less calibration because fundamental qualities such as displacement or strain are measured, and then used to obtain residual stress quantities [35]. Measuring residual stress using a destructive method consists of removing a section of the part and then measuring the deformation of the surrounding area that results from this material being removed. Calculations can then be performed to discover the residual stress that was present in the section that was removed. The method that will be utilized in this work is called the slitting method. For the slitting method, a cut is introduced into the part by a thin saw blade, milling cutter, or wire EDM [35]. A benefit of using the slitting method in contrast to other destructive methods is that the slitting method provides the user with a profile of the residual stress throughout the entire depth of the part. The residual stress perpendicular to the cut can be determined by measuring the deformation that is experienced when the slit of material is removed. Figure 21 shows a thin wall printed with LENS that has the slit for measuring the stress using the slitting method.

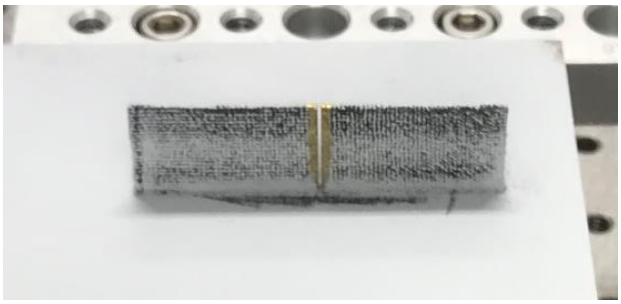

Figure 21 3D printed thin wall with slit cut in it for measurements using the slitting method.

The most common way of measuring the relaxation displacement for the slitting method is by using strain gauges. However, for this thesis Digital Image Correlation (DIC) was employed to make the measurements. DIC is an innovative technique for measuring strain and displacement optically using cameras. DIC compares digital photographs of the test piece at different stages of deformation. Software is then employed to compare blocks of pixels from the photographs at the different stages and uses them to measure surface displacement [36]. The displacements that are measured can then be used to determine the residual stress that was present in the removed section of the 3D part. Many of the software packages can even divide the displacement seen into three cartesian directions. An example of a surface displacement map that describes the displacement in the z-direction (height of the 3D build) is shown in Figure 22.

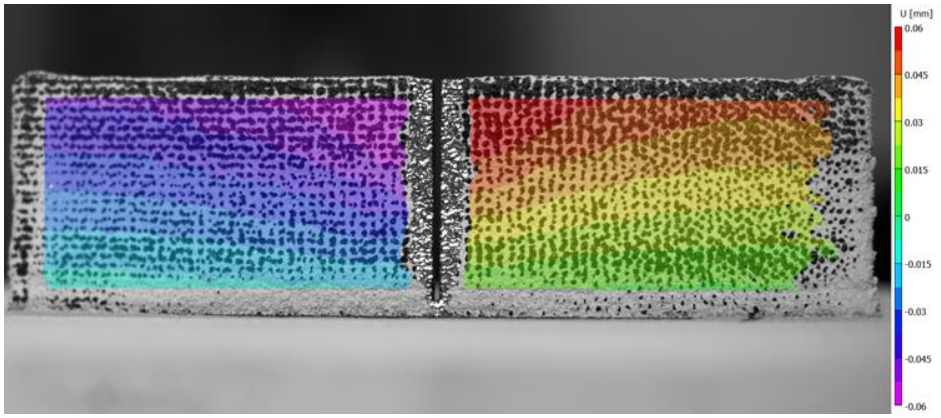

Figure 22 Displacement map that shows displacement in the height of the thin wall after slit is cut with wire EDM.

The setup that was used for the DIC portion of this work consisted to two major components. The first component was a fixture that is used to position the 3D printed part and the substrate in the same location before and after the slit is cut into it. The second component is the is the cameras that are used for the imaging. For this work, two 12 MP point grey grasshopper cameras with 17mm Schneider lenses were used (Figure 23).

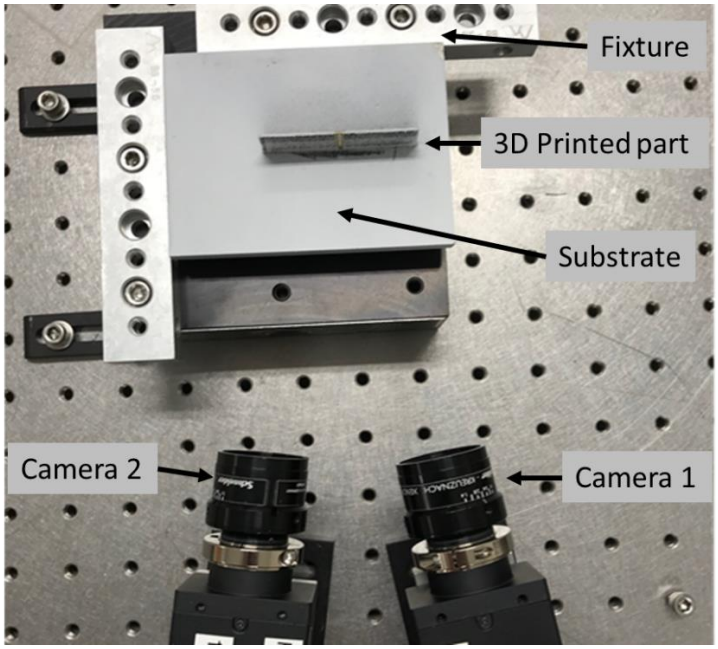

Figure 23 Setup used for DIC image processing.

The 3D printed metal parts that were manufactured for the slitting method were a different geometry than the parts used for the substrate warping method. For the slitting method, the 3D metal parts were thin walls that were 2in x 1in x .05in. The thin wall geometry used in these parts was selected to limit the residual stress to two dimensions, length and height of the wall. Table 2 shows other process settings that were used in printing the thin wall geometry used for the DIC method. These test parts were built at 5 different substrate temperatures, no substrate heat input, 150°C, 250°C, 350°C, and 450°C so comparisons could be made on how substrate temperature affects the residual stress. Three samples were printed at each of the 5 temperatures.

Table 2 LENS processing parameters for slitting method

Laser Power	400[W]
Powder Feedrate	6.5 [g/min]
Layer Thickness	0.25 [mm]
Hatch Spacing	N/A
Parameter Deposition Speed	400 [mm/min]
Infill Deposition Speed	N/A

Chapter 5 Results

This chapter documents the data that was collected during the experimentation using method 1, the substrate warping method, and method 2, the slitting method. Substrate deformation, and digital image correlation were used to determine residual stress at various levels of bed heating. Measured substrate and deformation for method 1, and printed part deformation for method 2 was collected for parts printed at a range of preheat conditions. This chapter will show the results from these experiments and process controls that can be used by designers and predictive modelers to aid in minimizing residual stress.

5.1 Method 1 – Substrate Warping Method

Data Collected from the substrate warping method experiment suggest that substrate temperature influences the amount of residual stress build up in a LENS manufactured part. The substrate with a 3D printed metal block that was manufactured without substrate heating experienced the greatest degree of warping as compared to substrates with substrate preheating. Substrate distortion measurements (Figure 24) show decreased warping with increased substrate preheat temperature. Since

residual stress buildup in LENS parts manifests itself through warping of the substrate, it is believed that heating the substrate allowed for stress relaxation in the part, therefore warping the substrate less.

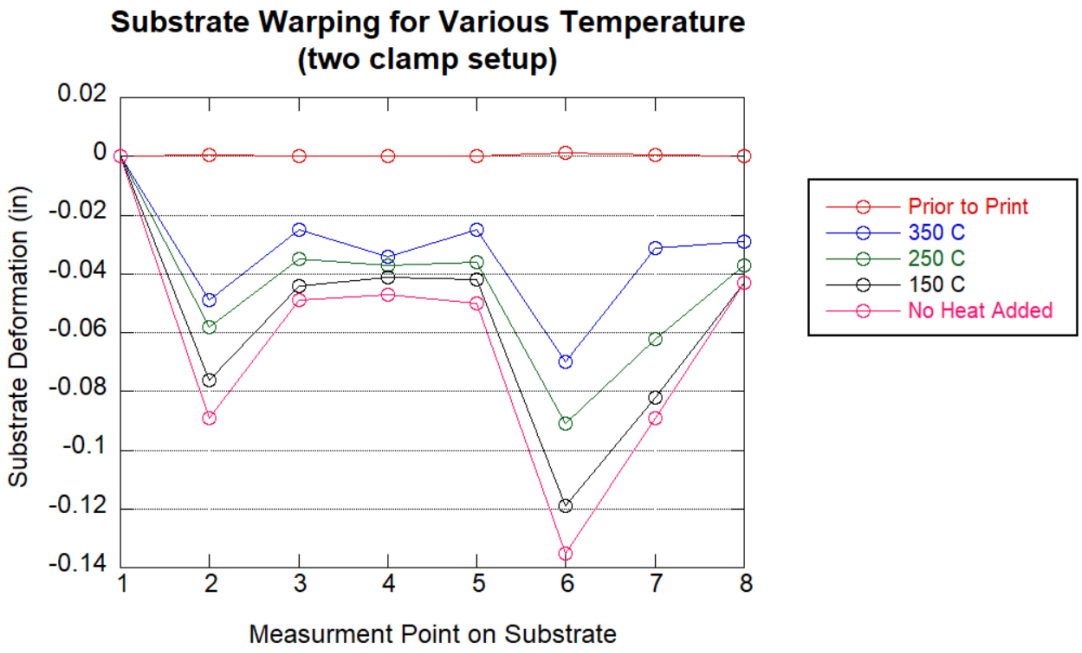

Figure 24 Substrate warping that was experienced at various temperature settings. All substrates were measured with an indicator, and point 1 was set as zero on all samples.

From this initial study, a trend is shown where increased temperature reduces substrate warping and residual stress buildup. As the 3D metal parts for this study were being manufactured, it was observed that within the first few layers of the block being built, that the residual stress was high enough to cause the substrate to warp. The warping that was observed caused the substrate to lose of contact with the heated platen. This observation of early print warping gave

rise to question what the actual temperature of the substrate was. Combining the observation of early warping with the simulation described previously in chapter 3.1 of this thesis, conclusions were made that the temperature of the substrate was likely much lower than desired. To mitigate the negative effects of early substrate warping more 3D parts were printed using a six-clamp configuration (Figure 20b). Figure 25 compares the warping of the substrate that had a part printed at 250℃ and a substrate that had a part printed at 250℃ with the extra clamping.

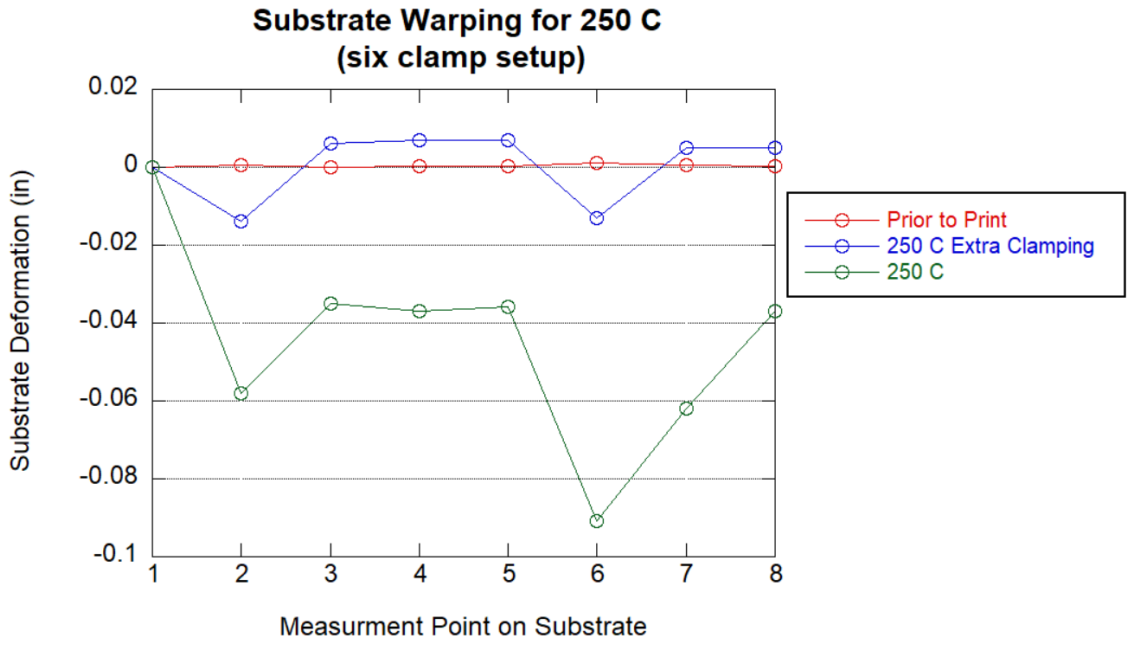

Figure 25 Substrate warping that was experienced at 250℃ with the normal clamping method, and with extra clamping. All substrates were measured with an indicator, and point 1 was set as zero on all samples.

The data in Figure 25 demonstrates when more clamps are used, there is less warping of the substrate. The six-clamp configuration held the substrate in contact with the heated print bed. The intimate contact that is maintained between the heated platen and the substrate provides a direct path for heat power to flow into the 3D printed metal part. The additional heat reduces enough stress that the deformation experienced at all the 8 measurement points is at least 1/5 the magnitude. For example, at measurement point 6 the substrate with 2 clamps deforms 0.091 inches, however the same point on the substrate with 6 clamps only deformed 0.013 inches. Another possible explanation for the decrease in substrate deformation in the case of extra clamping is that the clamps physically prevented the substrate from deforming, forcing the stress to manifest itself in other ways. This initial substrate warping experiment showed a trend that as more heat energy is added to the printed part through the substrate, less deformation is measured.

5.2 Method 2 – Stress Relaxation Method

Like the substrate warping method, the material cutting method suggests that temperature influences the accumulation of residual stress in 3D printed parts. The displacement maps

generated from DIC show the component of the displacement vector that is in U direction. Figure 26 shows the coordinate system used for DIC measurements, with the V direction in the image being the height of the part that was built. The U, or longitudinal direction of the 3D part, is the component of displacement that is along the length of the wall perpendicular to the slit (Figure 26). Because the slitting method is generally only used to determine stress perpendicular to the slit, only the U direction will be discussed in this chapter. The deformation of the printed sample is represented by colored overlay on the DIC image. The color code represents a range of deformations from positive to negative, so not only magnitude, but also direction can be determined from a DIC plot (Figure 26).

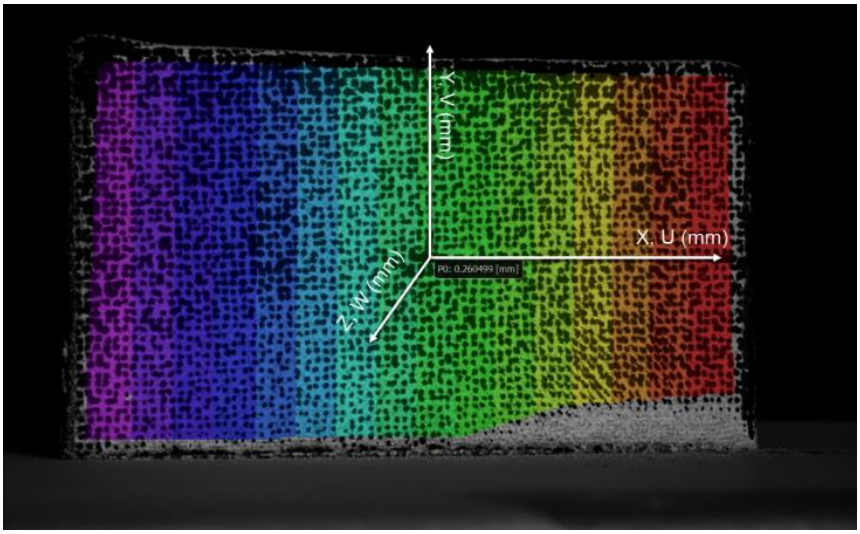

Figure 26 Example DIC deformation map with U, V, and W cartesian coordinate label.

For the thin wall geometry that was used for this study, the maximum displacement is along the top of the wall on all samples. On each side of the slit the displacement is in opposite directions with the slit opening wider as the material in the slit was removed. The slit opening wider suggests that the material that was removed in the slit had residual stress that was in tension. The observation of tension in the length of a thin wall geometry is characteristic, and what would be expected from a molten pool of metal solidifying layer by layer. DIC measurements taken in this study are of the 3D printed part still attached to the substrate. The slit that is cut into the part goes through the height of the deposition, and stops about 2mm from the substrate.

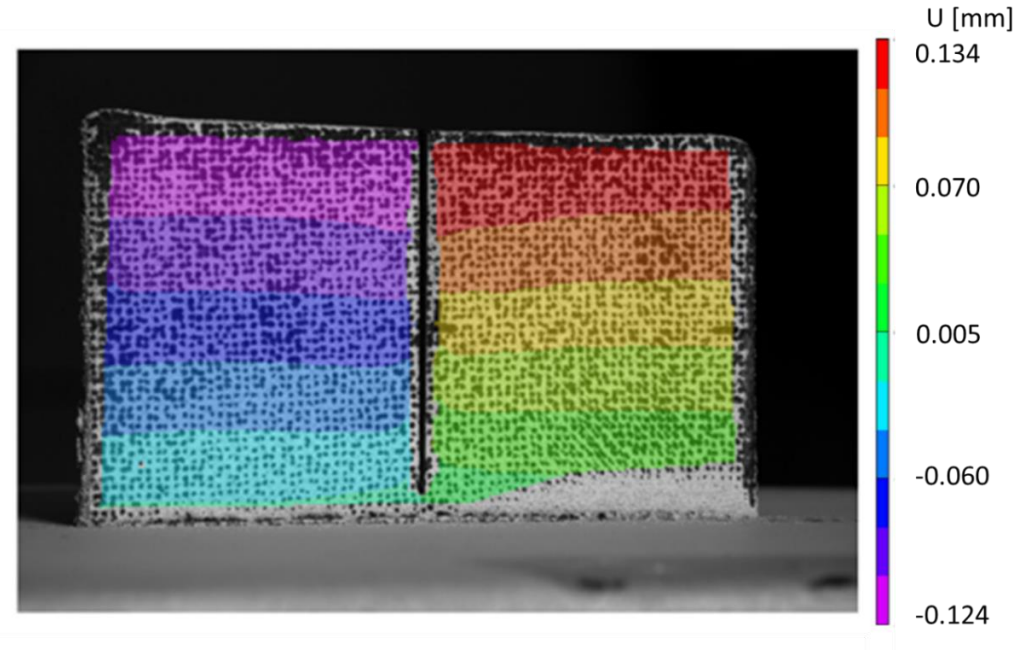

Figure 27 DIC deformation map of part printed at room temperature

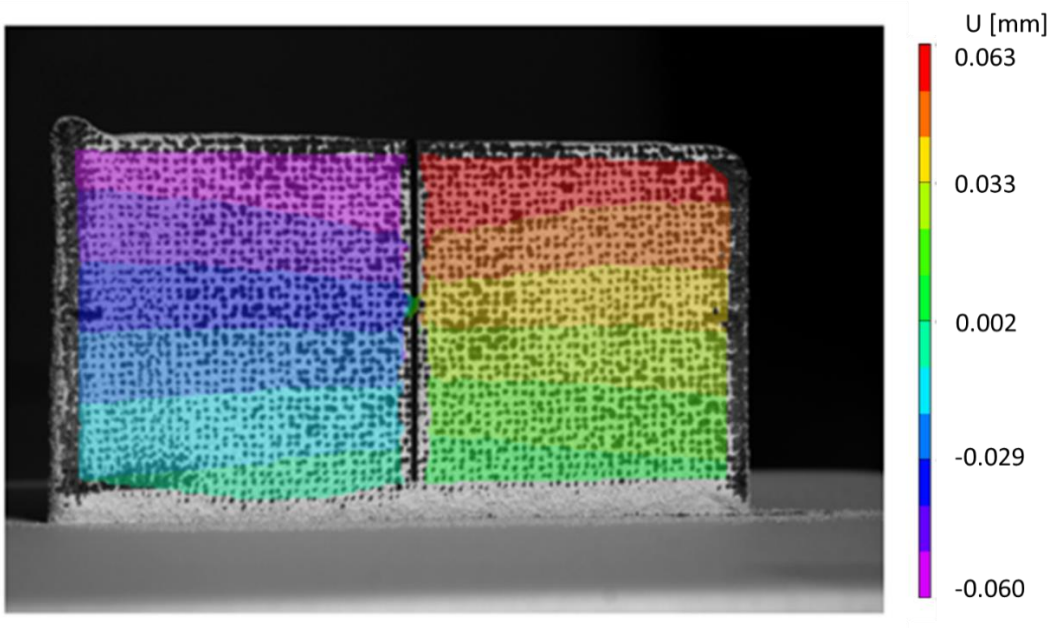

Figure 28 DIC deformation map of part printed at 450

The thin wall 3D parts that were printed at room temperature had displacements characteristic of Figure 27 after the slit was cut into the thin wall. The 3D parts printed at 450°C produced very similar displacement maps, however the magnitude of the displacement was much smaller than the parts at room temperature. The 3D parts printed at room temperature (Figure 27) had a maximum displacement of 0.134mm. However, the thin wall part that was printed at 450°C (Figure 28) experienced much smaller displacement of only 0.063mm. The smaller displacement indicates that the residual stress was significantly reduced by printing the AM part at the higher temperature of 450°C. To visualize the trend of how temperature changes the residual stress in a 3D printed part,

the data from the stress relaxation method was plotted in Figure 29. This plot shows us the same trend that was seen in Figure 24, which demonstrates that as temperature increases, the deformation measurement decreases. Both the substrate warping method, and the stress relaxation methods show that additional heating through the print platen provide a 3D printed metal part with less residual stress.

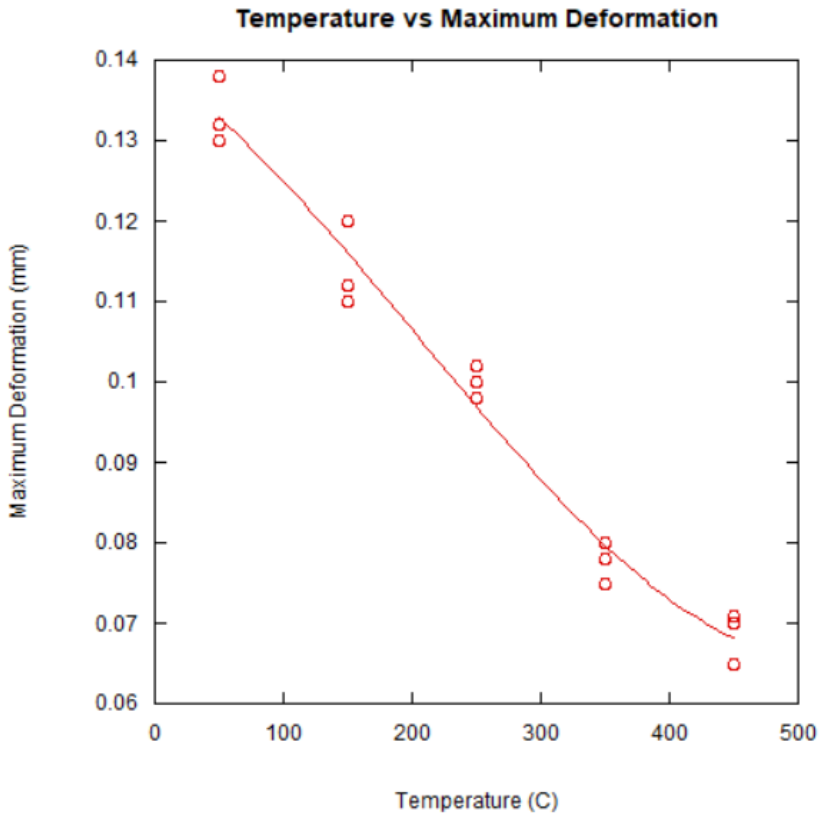

Figure 29 Plot of how DIC maximum deformation measurements change with temperature

Chapter 6 Conclusions and Future Work

6.1 Conclusions

Conclusions that can be drawn from this work are: First, the orientation of the 3D part on the substrate changes the thermal gradient and the maximum temperature that the part experiences. Second, it is important, at least with stainless steel, that the substrate and the heated platen remain in intimate contact with each other to maximize thermal input. Third, the heating the 3D part reduces stress that is developed in 3D printed parts by minimizing the thermal gradient, and reducing the cooling rate of the melt pool.

To display the significance the conclusions from this work have in making higher quality 3D printed metal parts, a demonstration was conducted. In this demonstration two samples were created by using LENS to print a pad on 0.030" shim stock. One sample was printed using minimal clamping and no heat added through the substrate. This first sample shows large amounts of deformation due to residual stress (Figure 30a). The second sample was printed using a picture frame clamping configuration, and a 450℃ platen temperature. This second sample shows significant reduction in warping, and is

considered a good quality part (Figure 30b). The application of the conclusions discussed in this show significant reduction of residual stress, and improvement in the quality of the produced 3D parts.

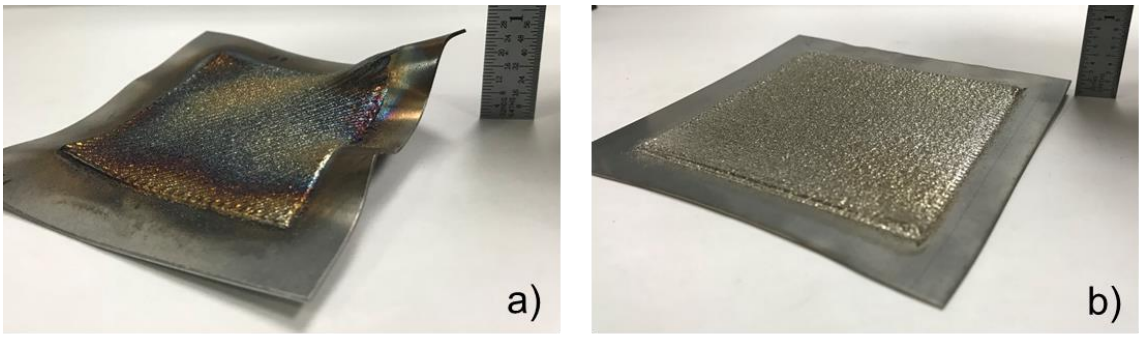

Figure 30 Conclusions demonstrator - 3-layer pad on 0.030" shim stock a) No added platen heat. b) Platen temperature of 450°C.

6.2 Future Work

The methods shown in this thesis have focused on deformation, that is a result of residual stress, however no methods have been shown to make calculations to determine numerical values for the stress. The current method being perused to measure the residual stress uses a model that takes the DIC measurements shown in this thesis, and puts them into PDE-constrained optimizer. This optimizer is then used to invert for the distribution of tractions on the cut plane, which can then be used to infer the relaxed stress distribution

throughout the entire volume of the remaining (non-sacrificial) material from the 3D part. Future work should consist of finishing the work to solve for the 3D stress distribution throughout the part.

Other future work should include answering many of the questions that have been brought up during this thesis. It is necessary that we learn how part orientation on the substrate changes the stress that is experienced. Good clamping, and amount of preheating both play a role in the stress development, but it is important that we learn what the relationship between them is. It is crucial that we develop an understanding of how preheating changes the microstructure and other properties of the materials that are printed. There are some materials that cannot currently be printed on LENS because they are too brittle and cannot print without cracking. If these brittle materials can be brought to a temperature above a glass transition temperature to relieve stress, experiments should be performed to try to print them that way.

6.3 Impact

This work was done on a LENS 3d printer, but has direct applications to many other print technologies as well. Additive manufacturing is a field of manufacturing that is here to stay. It is necessary to understand how to reduce negative aspects of 3D printing such residual stress. It is important that solutions are found to reduce negative characteristics of the technology rather than compensating for and then ignoring them like the industry currently does in many cases. This work will have direct impact our ability to reduce warping and increase our ability to print more materials.

From a broader perspective, this work will also increase the ability to create additively manufactured parts that can withstand the harsh environments experienced by the aerospace and defense industries. Currently a designer can define the limits of a part created using conventional manufacturing methods. Because there are so many variables and knobs that can be turned in additive manufacturing processes, the understanding of how a change in print parameters changes the properties of a 3D part is not fully understood. Currently there are many FEA models available that can predict residual

stress and microstructure of 3D printed parts. As the stress relief techniques discussed in this thesis are incorporated into modeling efforts, a greater understanding of how to produce AM parts with the desired properties will be developed. The largest impact comes when understanding of how a change in printing process variables impacts the properties of the resulting part, and can be applied to the design of parts that are optimized for production with AM technologies. The goal should be to improve predictive microstructure models and predictive residual stress models. Once improved these models should be combined with emerging technologies like topology optimization to define 3D part geometry, print settings, and the toolpath used for manufacturing. This procedure would allow additive manufacturing to provide the designer with alternative ways to produce the most complex and reliable parts that the world has ever known.

References

1. B.T.Wittbrodt, *Life-cycle economic analysis of distributed manufacturing with open-source 3-D printers.* Mechatronics, 2013. **23**(6): p. 713-726.

2. L.Wang, *Residual stresses in LENS-deposited AISI 410 stainless steel plates.* Materials Science and Engineering A, 2008. **496**(1-2): p. 234-241.

3. Rangaswamy, P., *Residual stresses in LENS® components using neutron diffraction and contour method.* Materials Science and Engineering A, 2005. **399**(1-2): p. 72-83.

4. Pratt, P., *Residual Stress Measurement of Laser-Engineered Net Shaping AISI 410 Thin Plates Using Neutron Diffraction.* Metallurgical and Materials Transactions A, 2008. **39**(13): p. 3155-3163.

5. *Lincoln Electric Preheating for welding explained.* 2018 [cited 2018 January 26]; Proffesionals guide to preheated welding]. Available from: http://www.lincolnelectric.com/en-us/support/process-and-theory/Pages/preheat-detail.aspx.

6. R.H.Leggatt, *Residual stresses in welded structures.* International Journal of Pressure Vessels and Piping, 2008. **85**(3): p. 144-151.

7. Tso-LiangTenga, *Effect of welding conditions on residual stresses due to butt welds.* International Journal of Pressure Vessels and Piping, 1998. **75**(12): p. 857-864.

8. Ali, H., *In-situ residual stress reduction, martensitic decomposition and mechanical properties enhancement through high temperature powder bed pre-heating of Selective Laser Melted Ti6Al4V.* Materials Science and Engineering: A, 2017. **695**(17 May 2017): p. 211-220.

9. Shiom, M., *Residual Stress within Metallic Model Made by Selective Laser Melting Process.* CIRP Annals, 2004. **53**(1): p. 195-198.

10. Griffith, M.L., *Understanding Thermal Behavior in LENS Proccessing of Structural Materials.* Sandia National Labs SAND Report, 1998. **SAND98-2475C**.

11. Smugeresky, J., *Investigation of Solidification in the Laser Engineered Net Shaping (LENSTM) Process.* Sandia National Labs SAND Report, 1999. **SAND99-1550J**.

12. Ye, R., *Numerical modeling of the thermal behavior during the LENS® process.* Materials Science and Engineering A, 2006. **426**(1-2): p. 47-53.

13. Yin, H., *Dendrite growth simulation during solidification in the LENS process.* Acta Materialia, 2010. **58**(4): p. 1455-1465.

14. Hofmeister, W., *Solidification in direct metal deposition by LENS processing.* Journal of the Minerals, Metals and Materials Society (JOM), 2001. **53**(9): p. 30-34.

15. Griffith, M.L., *Laser Engineered Net Shaping.* Sandia National Labs SAND Report, 2000. **SAND2000-2352**.

16. Y.C.Tsui, *An analytical model for predicting residual stresses in progressivelydeposited coatings.* Thin Solid Films, 1997. **306**(1): p. 23-33.

17. Keicher, D., *Metal Additive Manufacturing*, in *January 19 2008 10:15am-11:15am*, S. Whetten, Editor. 2018.

18. Bland, S., *Mapping out the additive manufacturing landscape.* Metal Powder Report, 2015. **70**(3): p. 115-119.

19. Additively. *Binder Jetting*. 2018 [cited 2018 January 22]; Available from: https://www.additively.com/en/learn-about/binder-jetting.

20. Do, T., *Process development toward full-density stainless steel parts with binder jetting printing.* International Journal of Machine Tools and Manufacture, 2017. **121**(October 2017): p. 50-60.

21. Ziaee, M., *Binder-Jet Printing of Fine Stainless Steel Powder with Varied Final Density.* Journal of Minerals, Metals, and Materials Society, 2017. **69**(3): p. 592-596.

22. Nandwana, P., *Powder bed binder jet 3D printing of Inconel 718: Densification, microstructural evolution and challenges.* Current Opinion in Solid State and Materials Science, 2017. **21**(4): p. 207-218.

23. Additively. *SLS*. 2018 [cited 2018 January 22]; Available from: https://www.additively.com/en/learn-about/laser-melting.

24. Frazier, W.E., *Metal Additive Manufacturing: A Review.* Journal of Materials Engineering and Performance, 2014. **23**(6): p. 1917-1928.

25. Smugeresky, J.E., *On the interface between LENS deposited stainless steel 304L repair geometry and cast or machined components.* Sandia National Labs SAND Report, 2004. **SAND2004-4035**.

26. Zhai, Y., *Novel Forming of Ti-6Al-4V by Laser Engineered Net Shaping.* Materials Science Forum, 2013. **765**: p. 393-397.

27. Keicher, D.M., *From the inside out: LENSfuels paradigm shift in modern manufacturing.* Metal Powder Report, 2000. **55**(9): p. 32-35.

28. Wang, L., *Analysis of thermal phenomena in LENS™ deposition.* Materials Science and Engineering A, 2006. **435-436**(5 Nov, 2006): p. 625-631.

29. Kwak, Y.-M., *Geometry Regulation of Material Deposition in Near-Net Shape Manufacturing by Thermally Scanned Welding.* Journal of Manufacturing Processes, 2002. **4**(1): p. 28-41.

30. *Stress relieving heat treatments for austenitic stainless steels.* [cited 2018 January 8]; Available from: https://www.bssa.org.uk/topics.php?article=76.

31. *Product Data Sheet – Stainless Steel Grades 304 vs 304L.* [cited 2018 March 3]; Available from: http://www.australwright.com.au/technical-data/advice/stainless-steel/grade-304-vs-304l/.

32. *Thermal conductivity of gasses.* [cited 2018 March 1]; Available from: https://www.engineersedge.com/heat_transfer/thermal-conductivity-gases.htm.

33. Spisz, E.W., *Solar Absorbtances and Spectral Reflectances of 12 Metals for Temperatures Ranging from 300 to 500 K* N.t. note, Editor. 1969.

34. Nonhof, C.J., *Material Processing with Nd-Lasers*. 1988, United Kingdom: Electrochemical Publications.

35. Schajer, G., *Relaxation Methods for Measuring Residual Stresses: Techniques and Opportunities.* Experimental Mechanics, 2010. **50**(8): p. 1117-1127.

36. McCormick, N., *Digital Image Correlation.* Materials Today, 2010. **13**(12): p. 52-54.

Appendix

A.1 Thermal Simulations for all studied temperatures

No heat added through platen

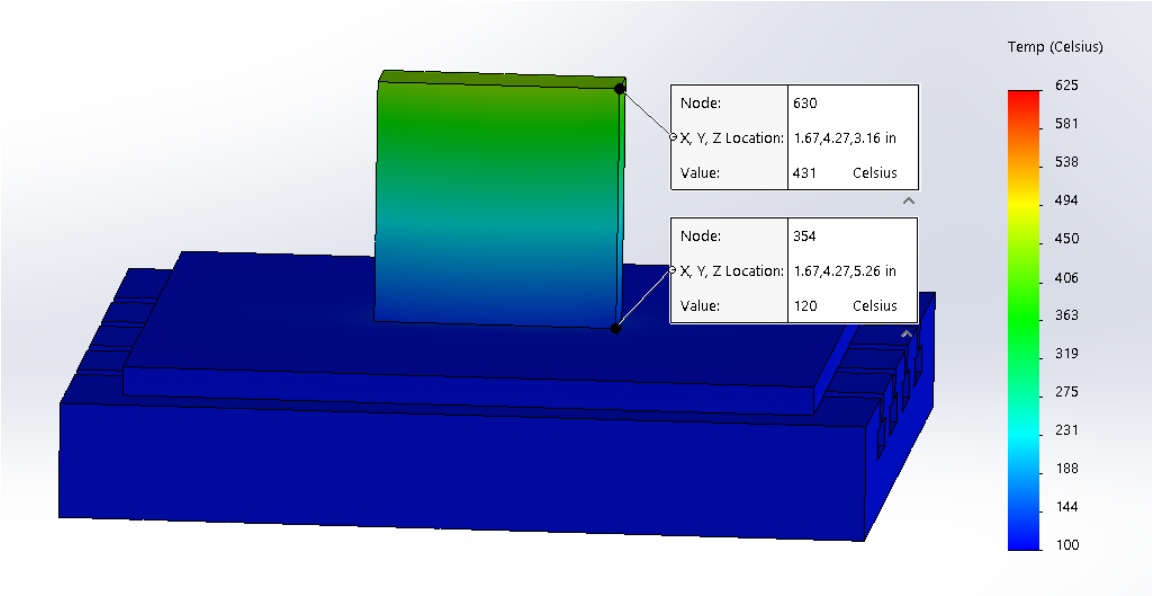

Platen temperature 150℃

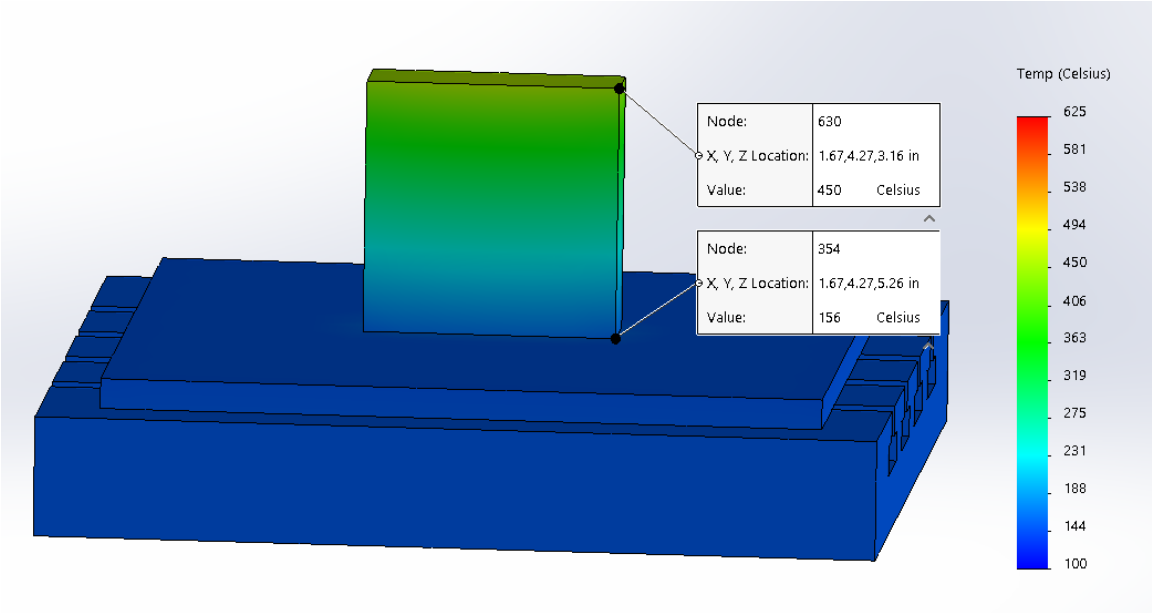

Platen temperature 250℃

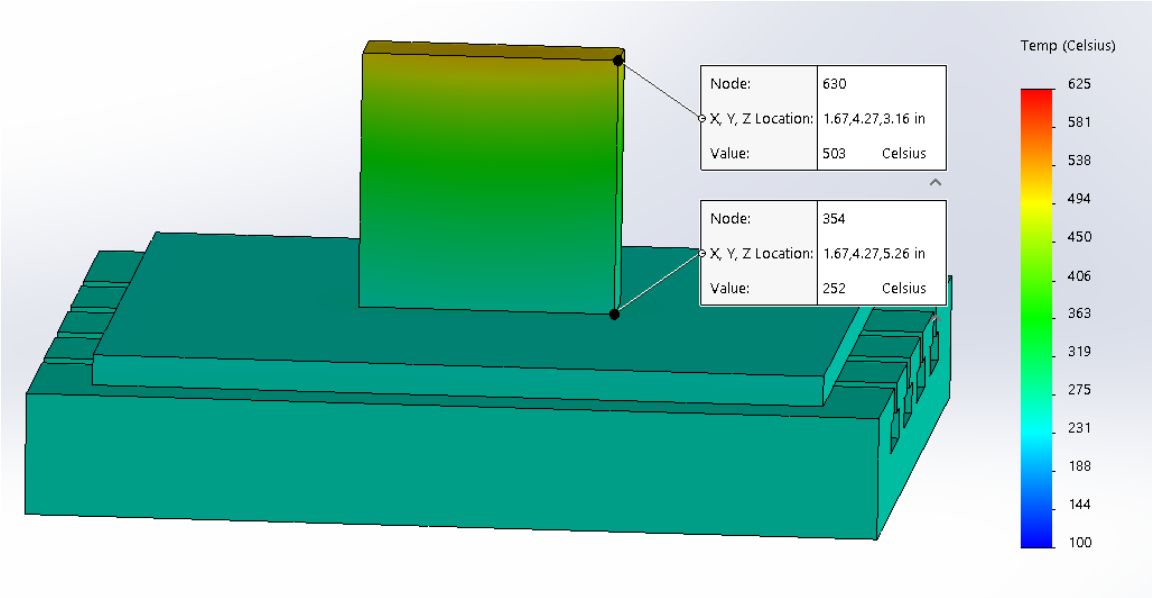

Platen temperature 350℃

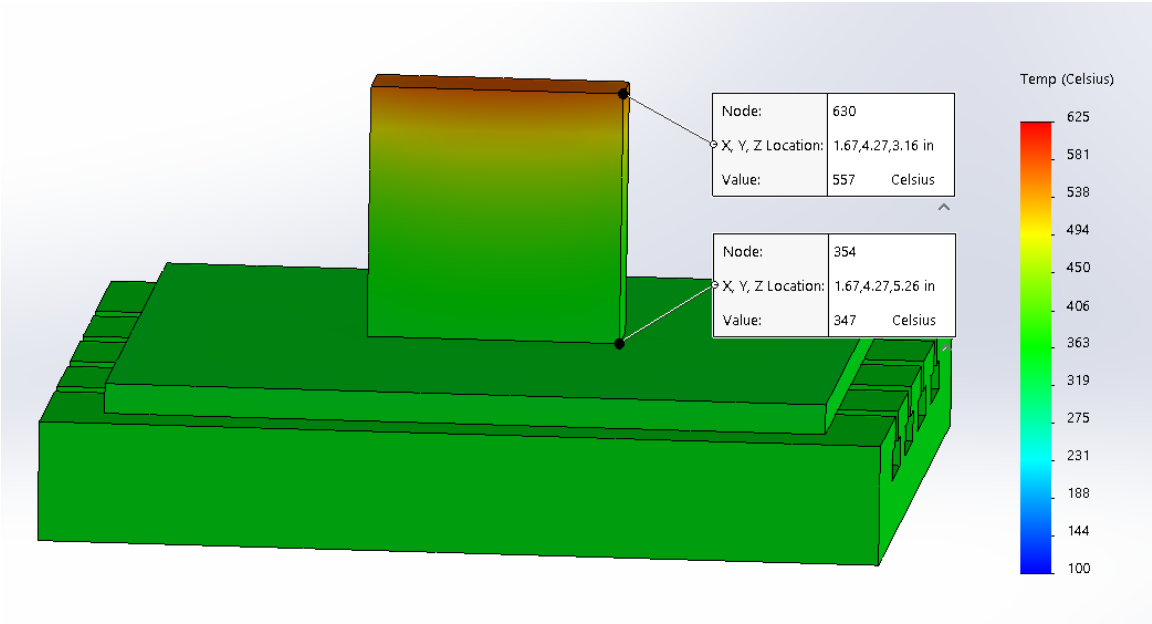

Platen temperature 450℃

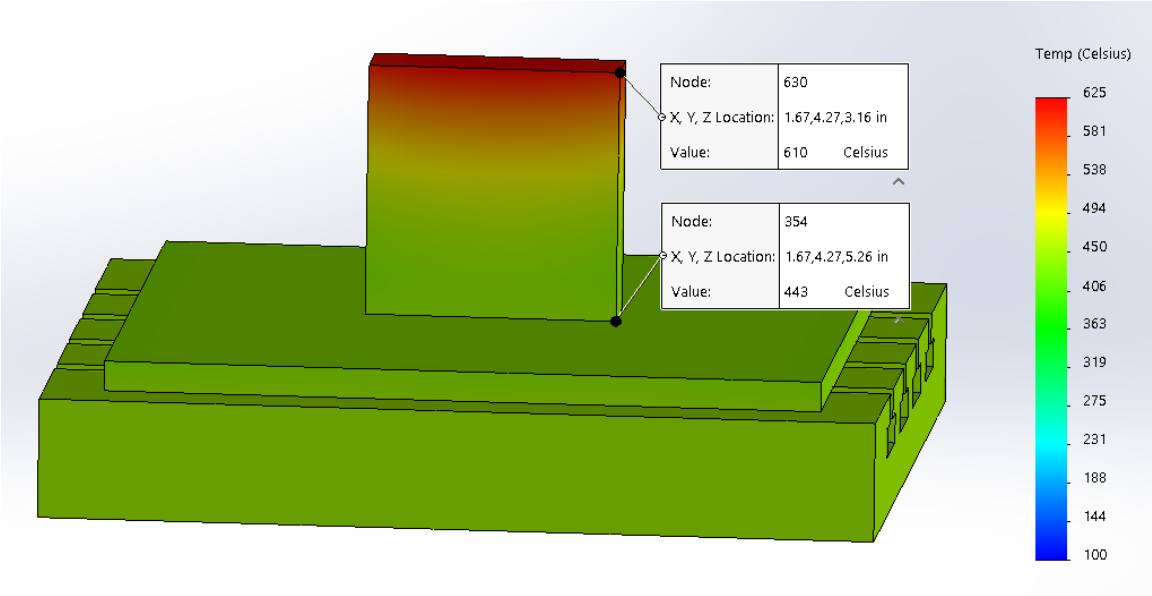

A.2 Spectral reflectance of metals at various wavelengths

[34]

Wavelength, μm	Spectral reflectance											
	Aluminum	Copper	Gold	Molybdenum	Nickel	Platinum	Silver	Stainless steel 304	Tantalum	Tin	Titanium	Vanadium
0.330	0.808	0.206	0.309	0.416	0.340	0.541	0.274	0.453	0.386	0.569	0.135	0.397
.354	.823	.220	.312	.417	.355	.563	.623	.475	.406	.602	.145	.417
.377	.835	.229	.325	.420	.411	.581	.688	.500	.407	.648	.150	.427
.398	.840	.261	.337	.434	.435	.611	.748	.523	.420	.701	.167	.449
.415	.848	.290	.338	.450	.463	.626	.782	.536	.410	.716	.168	.455
.430	.851	.317	.336	.466	.476	.636	.803	.546	.410	.749	.177	.464
.444	.855	.334	.340	.480	.498	.645	.835	.563	.408	.761	.186	.462
.457	.864	.348	.338	.488	.508	.651	.831	.568	.403	.783	.192	.468
.470	.863	.383	.344	.500	.520	.663	.843	.583	.407	.791	.199	.475
.483	.869	.396	.353	.507	.530	.667	.856	.583	.398	.809	.208	.474
.497	.863	.410	.447	.506	.539	.688	.883	.586	.403	.812	.212	.473
.511	.865	.448	.585	.510	.554	.711	.893	.594	.397	.817	.218	.472
.525	.865	.455	.680	.505	.556	.710	.903	.598	.386	.821	.214	.468
.540	.863	.463	.749	.511	.566	.724	.888	.602	.387	.818	.213	.472
.554	.870	.494	.794	.506	.571	.720	.913	.616	.387	.824	.236	.470
.569	.871	.580	.824	.507	.583	.719	.906	.616	.384	.843	.240	.476
.584	.871	.701	.852	.508	.591	.720	.936	.625	.384	.832	.244	.477
.599	.877	.757	.873	.504	.601	.730	[a].934	.627	.391	.830	.246	.471
.614	.870	.790	.890	[a].519	.597	.721	[a].940	[a].624	.398	[a].845	.250	[a].472
.630	[a].866	.784	[a].902	[a].520	[a].613	[a].737	.932	[a].638	[a].406	[a].830	[a].255	[a].480
.647	[a].872	.832	[a].922	[a].522	[a].626	[a].731	[a].958	[a].634	[a].431	[a].839	[a].274	[a].480
.665	[a].876	[a].840	[a].929	[a].530	[a].626	[a].743	[a].957	[a].640	[a].460	[a].836	[a].275	[a].484
.682	.881	.861	.946	.525	.635	.743	.977	.645	.490	.841	.281	.488
.701	.870	.869	.953	.545	.645	.770	.975	.651	.532	.835	.292	.489
.721	.876	.881	.943	.540	.647	.760	.984	.675	.564	.846	.297	.493
.743	.868	.848	.967	.535	.653	.765	.968	.670	.606	.853	.307	.500
.764	.860	.891	.967	.523	.655	.763	.963	.664	.632	.845	.320	.505
.788	.850	.898	.972	.535	.669	.762	.976	.666	.664	.840	.318	.501
.812	.849	.901	.968	.533	.671	.776	1.000	.671	.697	.824	.327	.504
.840	.834	.918	.973	.530	.674	.781	.983	.676	.720	.835	.336	.517
.868	.840	.918	.977	.540	.684	.778	.970	.680	.744	.824	.344	.510
.898	.873	.923	.980	.541	.684	.778	.978	.671	.772	.826	.333	.518
.929	.890	.945	.978	.557	.687	.778	.983	.684	.793	.840	.355	.528
.966	.914	.944	.990	.577	.660	.790	1.000	.676	.809	.820	.334	.518
1.003	.937	.940	.982	.602	.696	.805	.960	.695	.833	.824	.344	.523
1.045	.944	.949	.987	.636	.703	.801	.990	.700	.845	.820	.350	.530
1.085	.948	.960	.992	.723	.716	.816	.990	.699	.865	.815	.358	.542
1.130	.965	.957	.987	.769	.719	.810	.988	.695	.875	.815	.361	.562
1.180	.960	.960	.988	.789	.731	.808	.985	.720	.891	.820	.368	.572
1.240	.970	.975	.997	.775	.751	.815	.948	.720	.911	.839	.385	.612
1.300	.970	.970	.990	.779	.767	.822	.995	.726	.915	.853	.394	.620
1.380	.970	.971	.992	.824	.776	.820	1.000	.735	.933	.892	.402	.653
1.470	.984	.988	1.000	.870	.832	.850	1.000	.798	.961	.879	.433	.708
1.580	.988	.991	.995	.897	.850	.866	1.000	.814	.962	.905	.444	.733
1.710	.976	.980	.990	.881	.815	.826	1.000	.769	.949	.896	.441	.722
1.900	.971	.970	.985	.887	.810	.798	1.000	.756	.937	.891	.445	.723
2.160	.968	.975	.990	.906	.830	.812	1.000	.770	.948	.885	.461	.773

A.3 DIC data for all samples at various platen temperatures

Sample 1 50℃

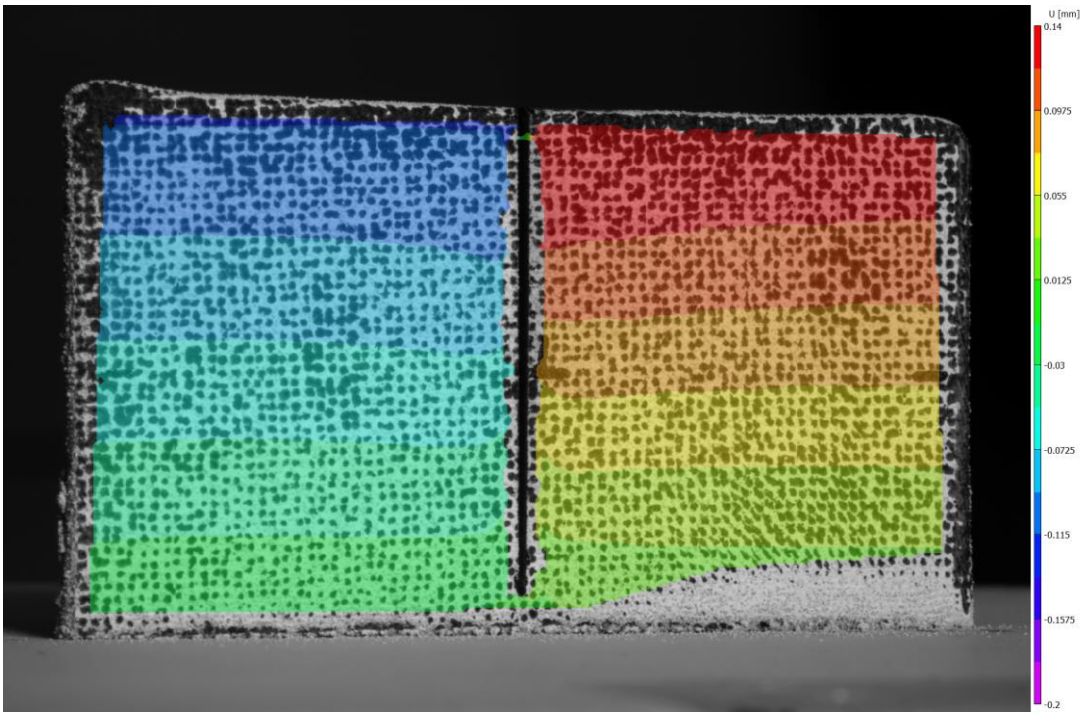

Sample 2 50℃

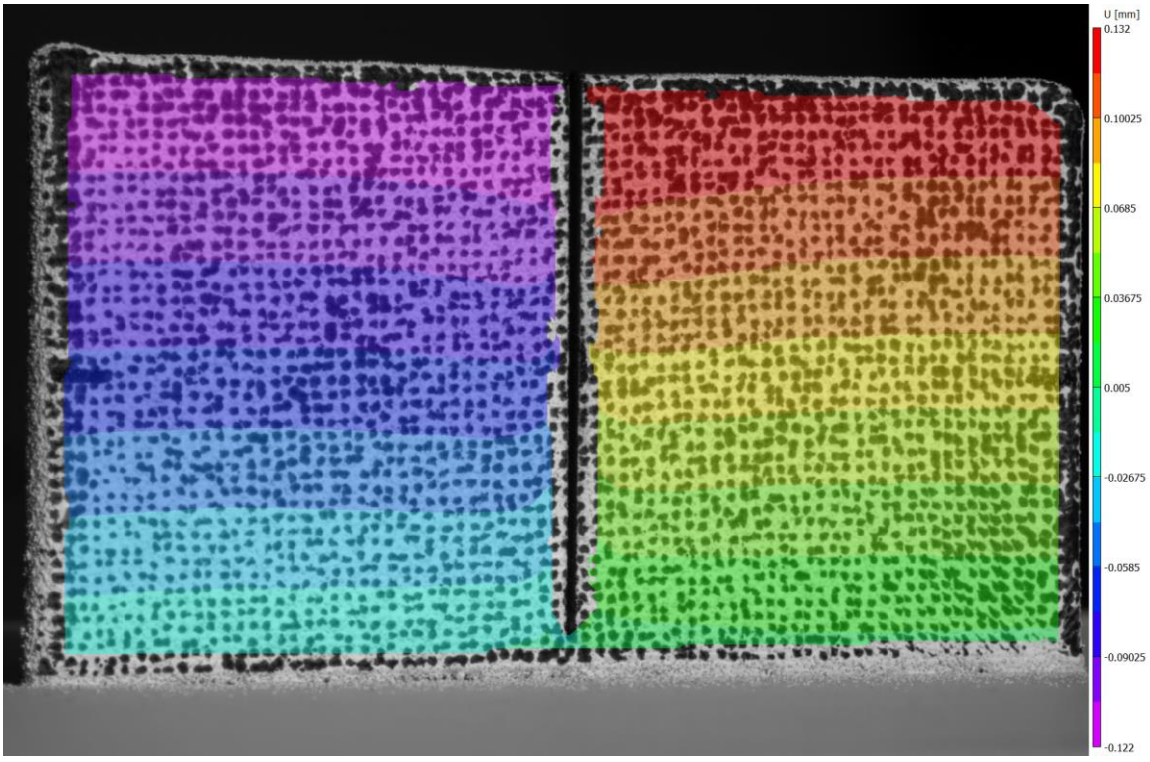

Sample 3 50℃

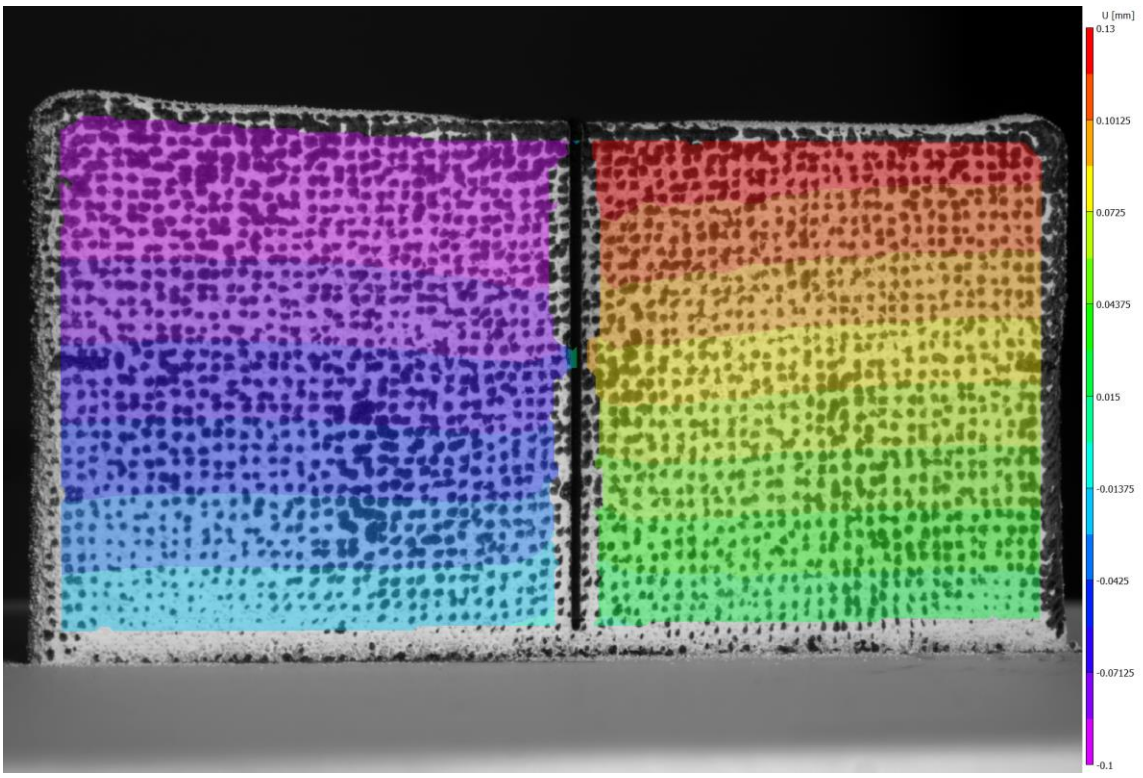

Sample 4 150℃

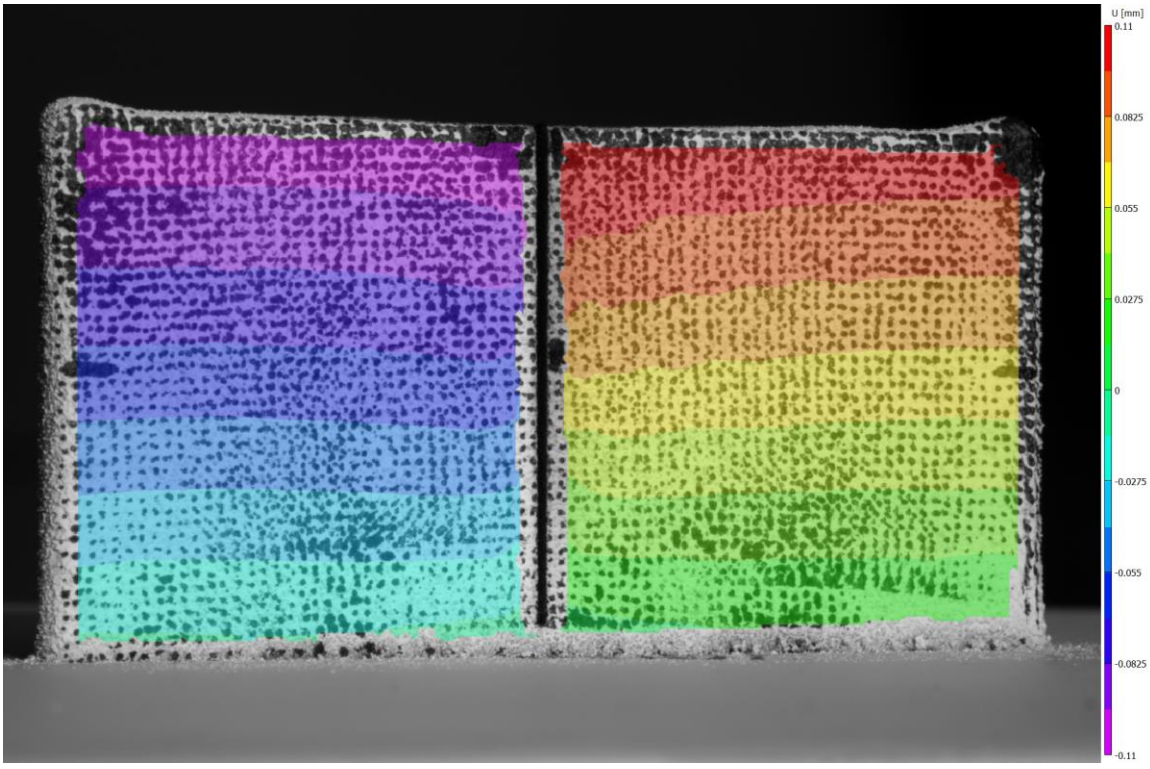

Sample 5 150℃

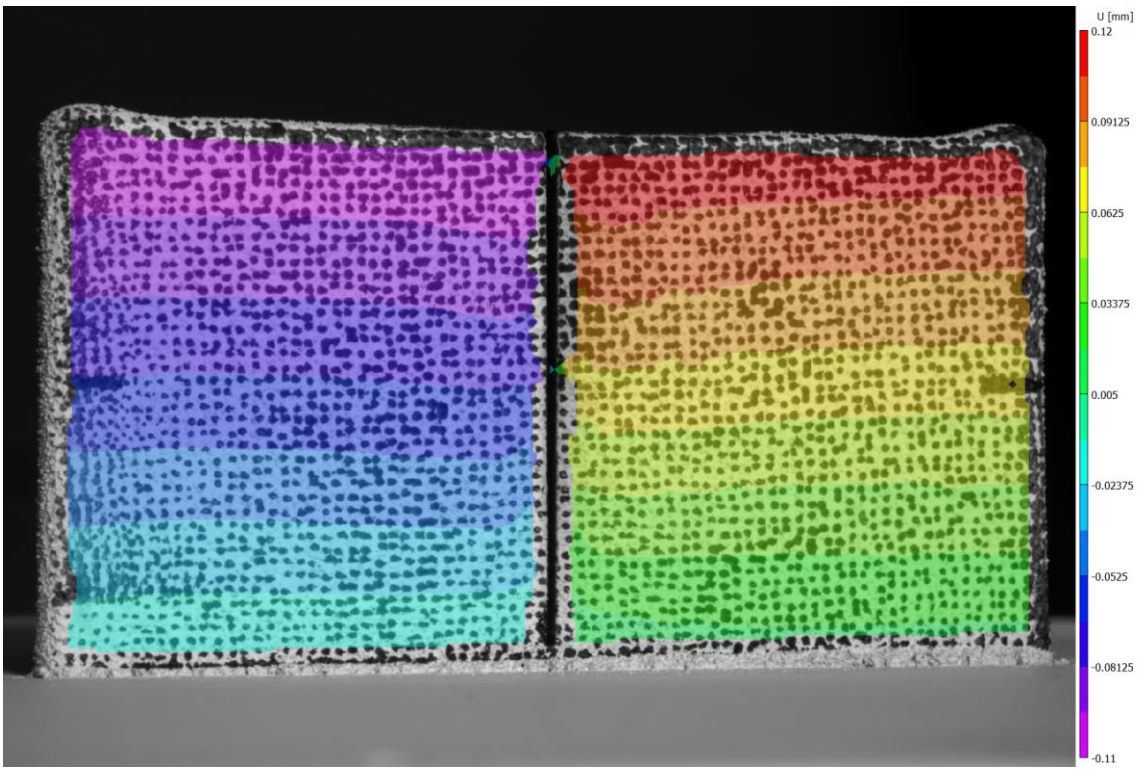

Sample 6 150℃

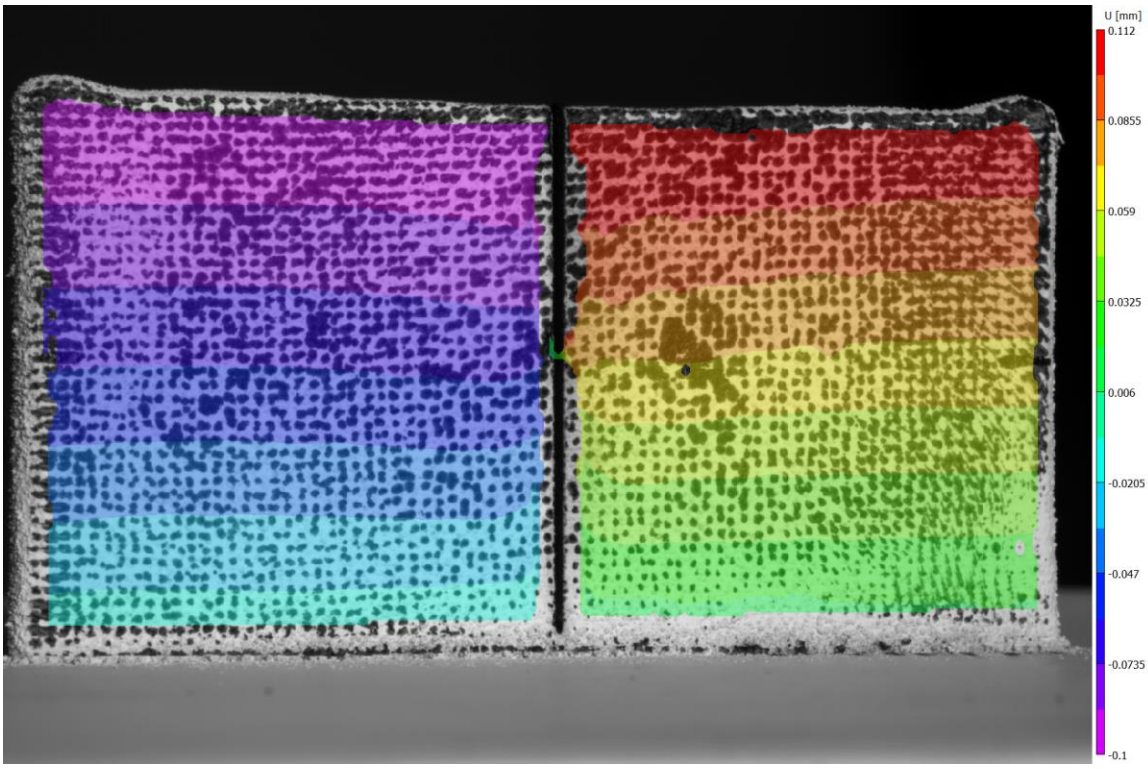

Sample 7 250℃

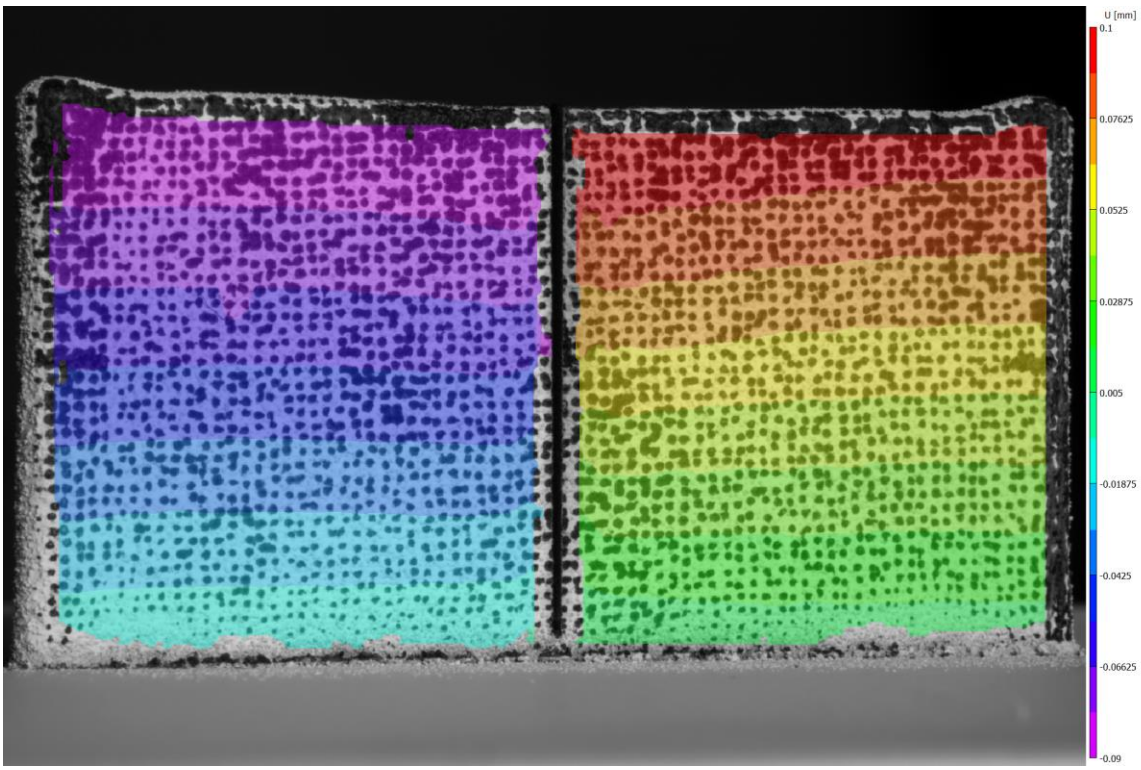

Sample 8 250℃

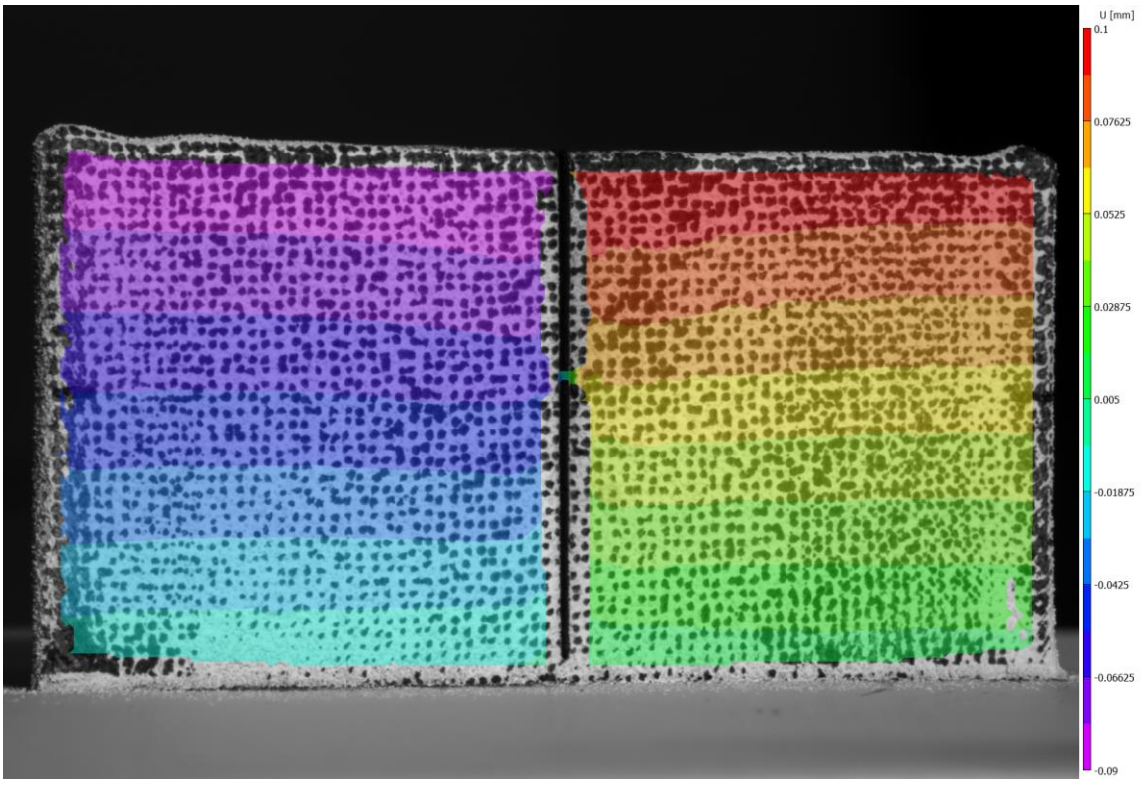

Sample 9 250℃

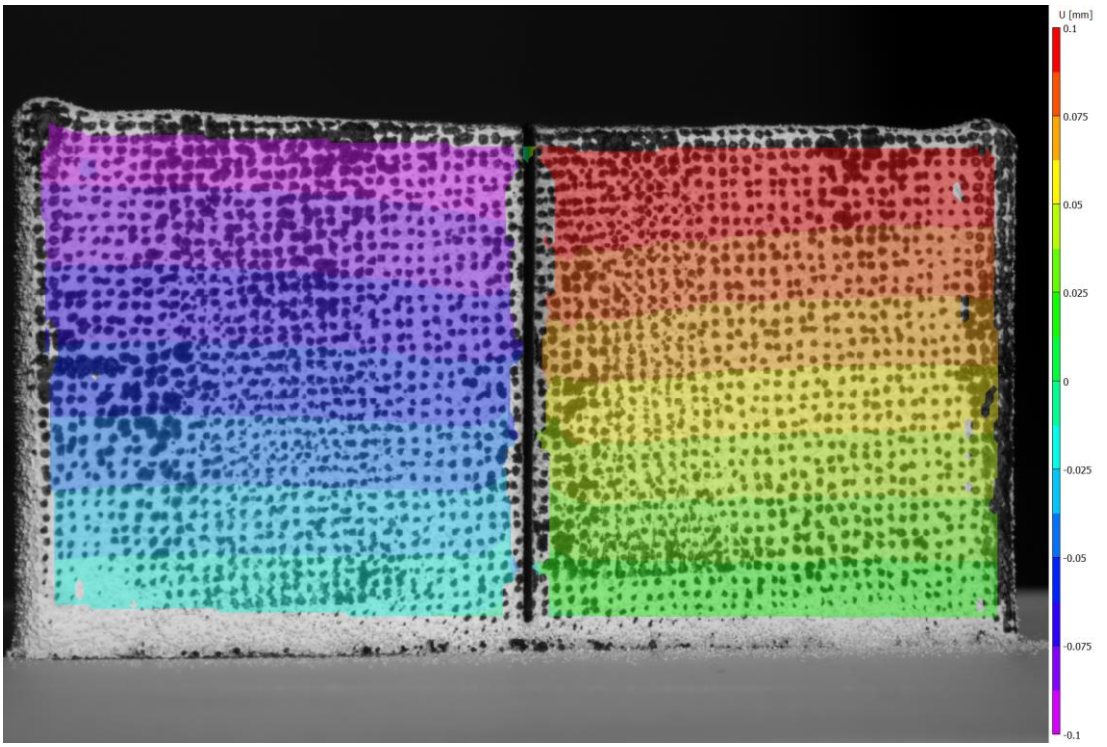

Sample 10 350℃

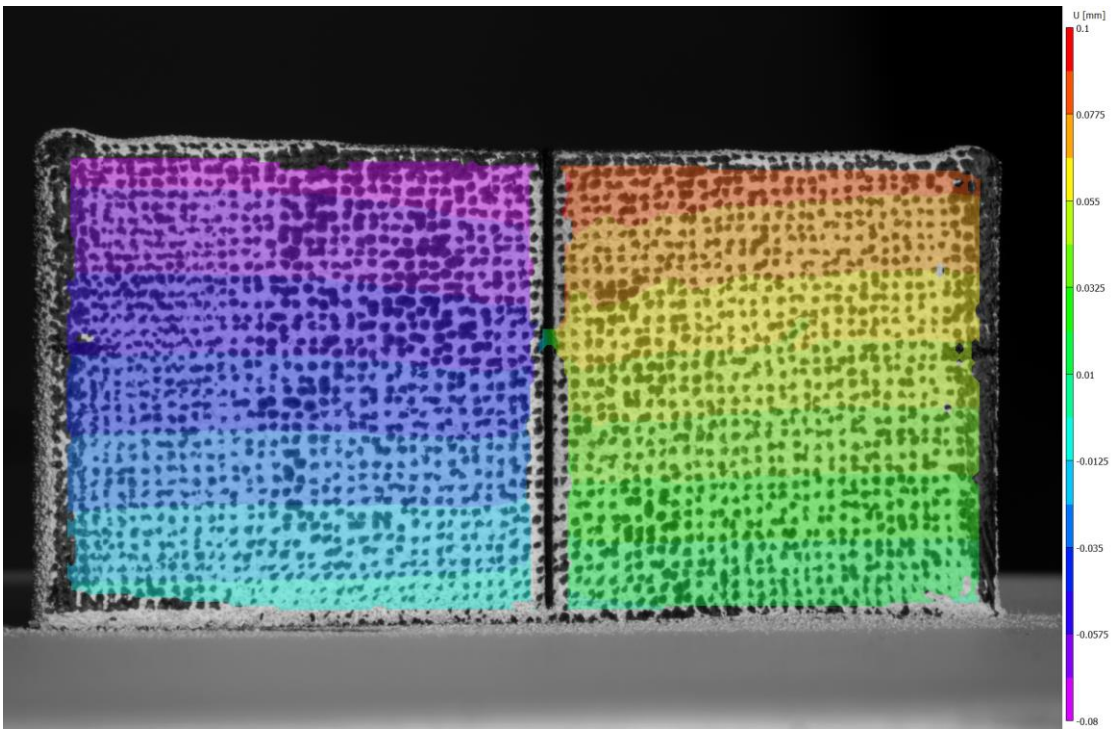

Sample 11 350℃

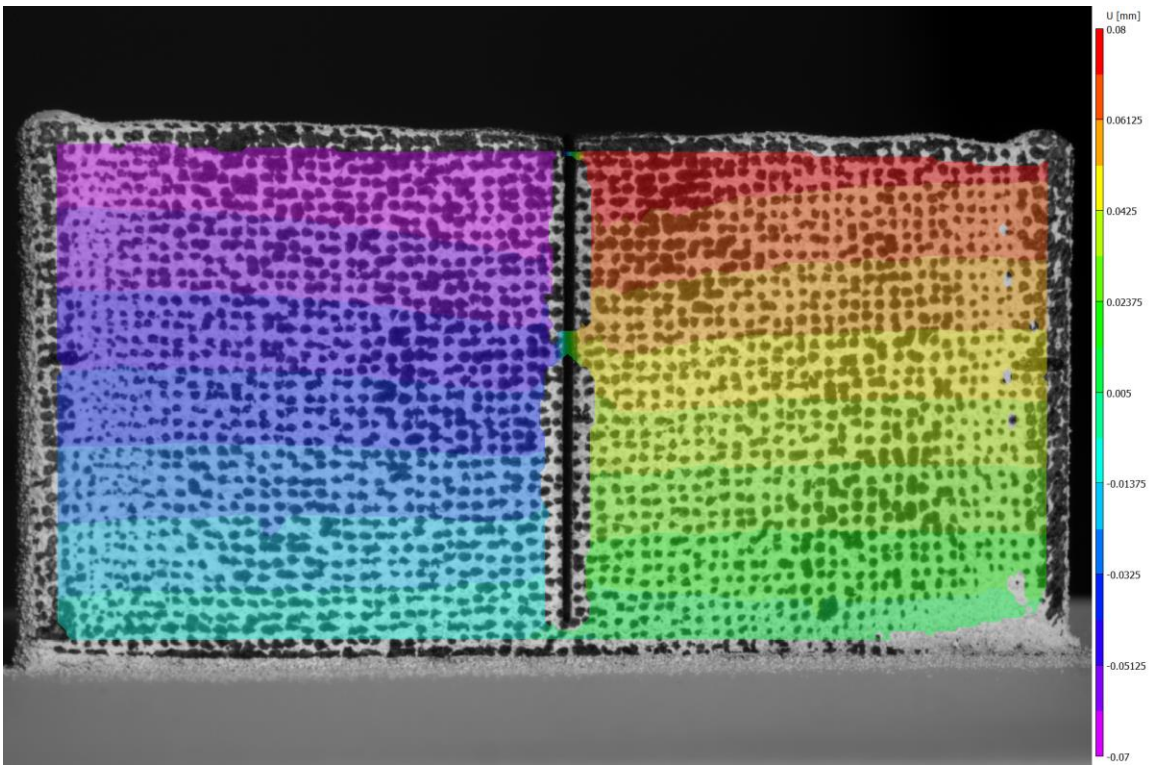

Sample 12 350℃

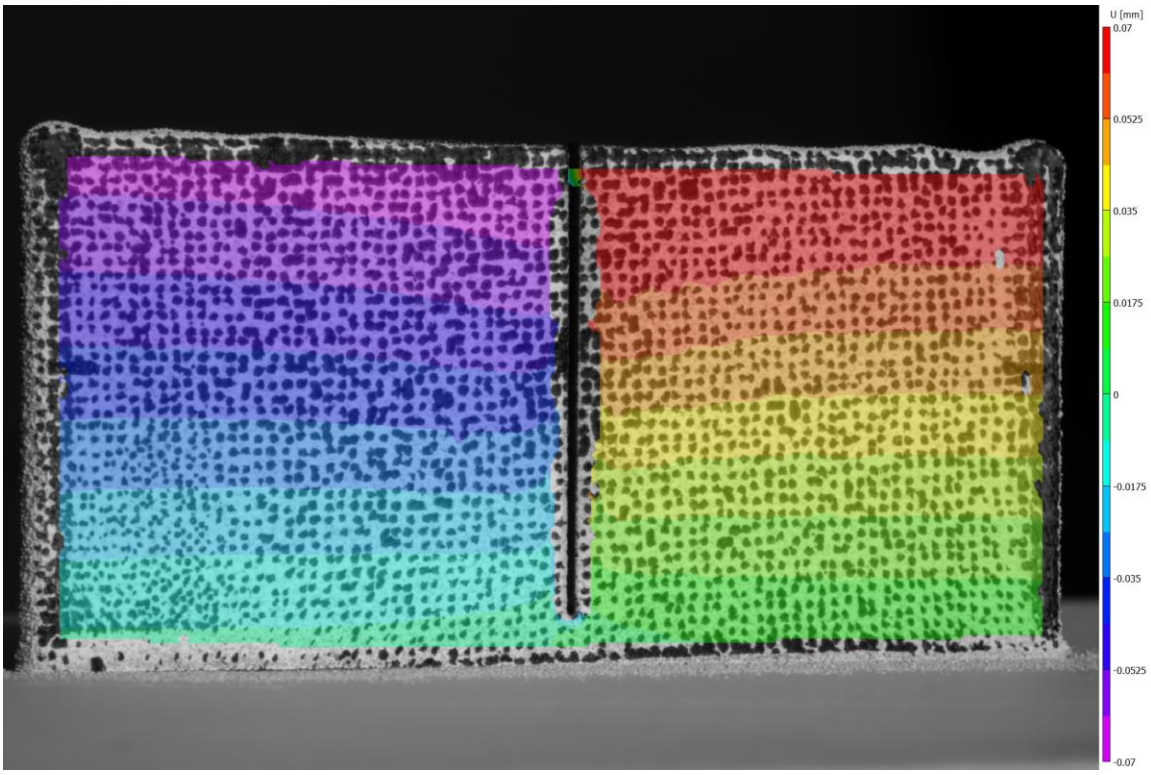

Sample 13 450℃

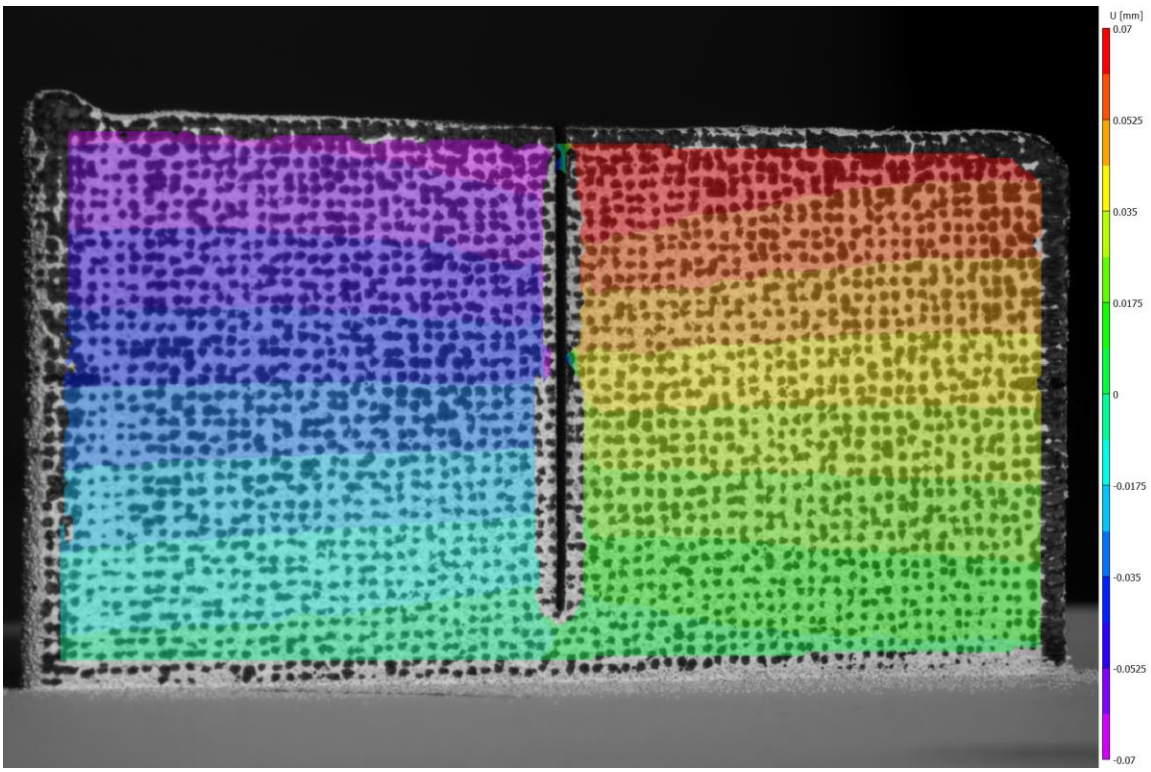

Sample 14 450℃

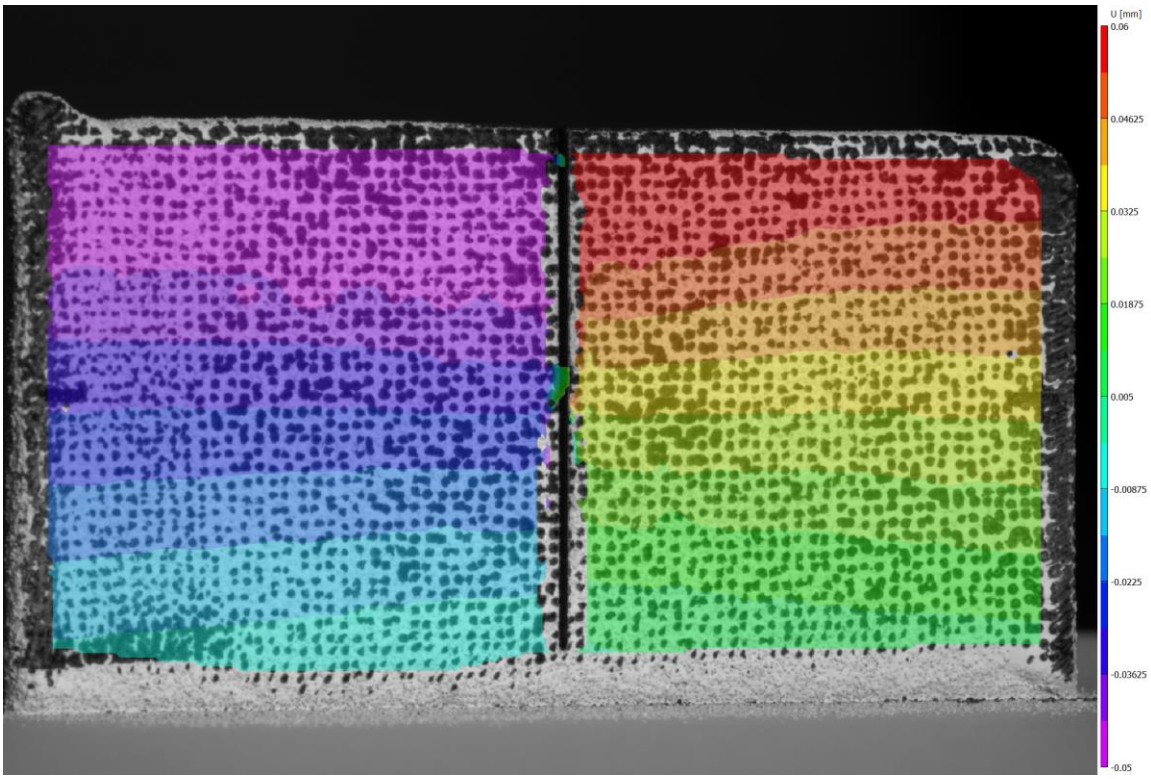

Sample 15 450℃

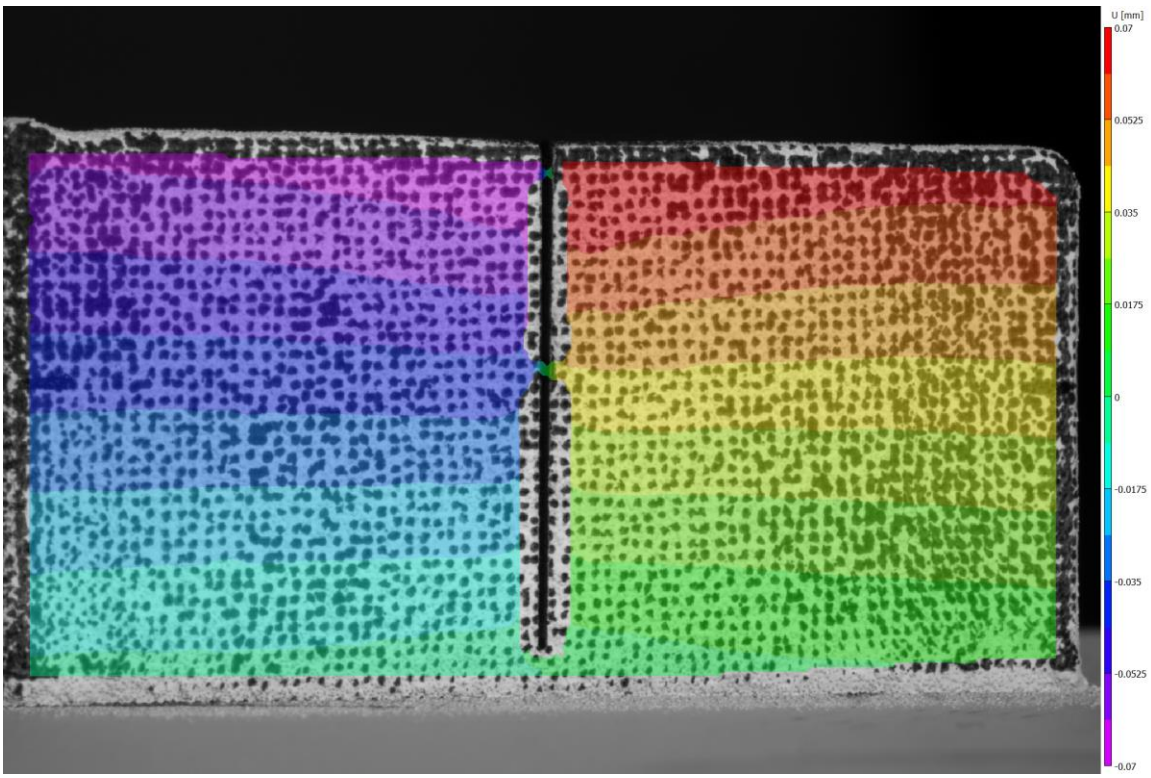

A.4 Measured temperature for each platen setting

Platen temperature during print with no heat added

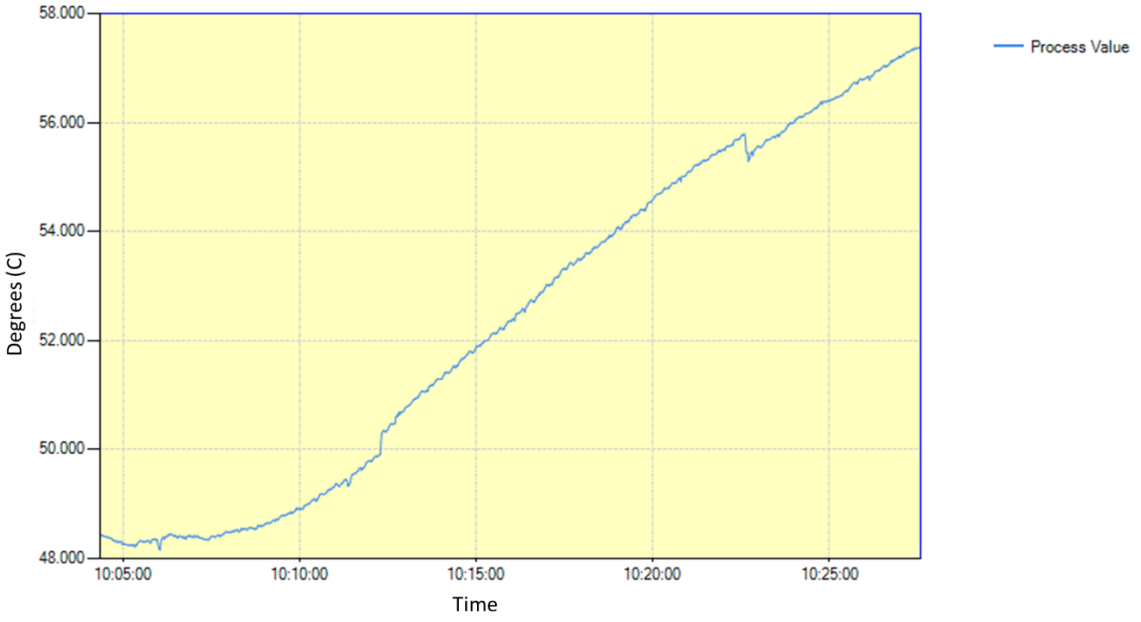

Platen temperature during 150℃ print

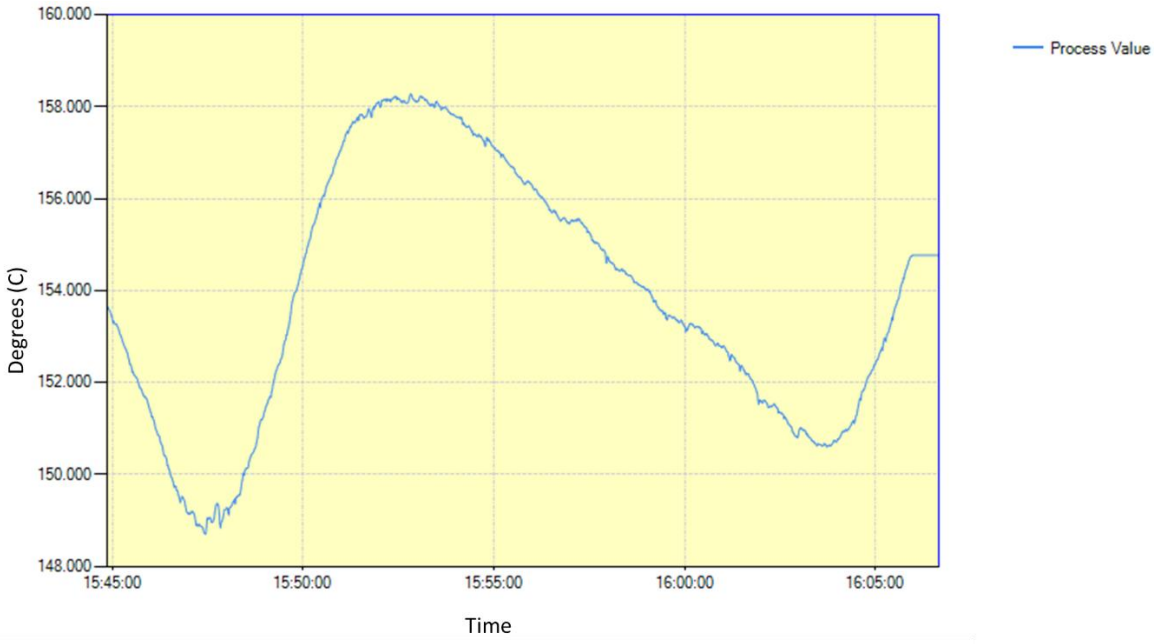

Platen temperature during 250℃ print

Platen temperature during 350℃ print

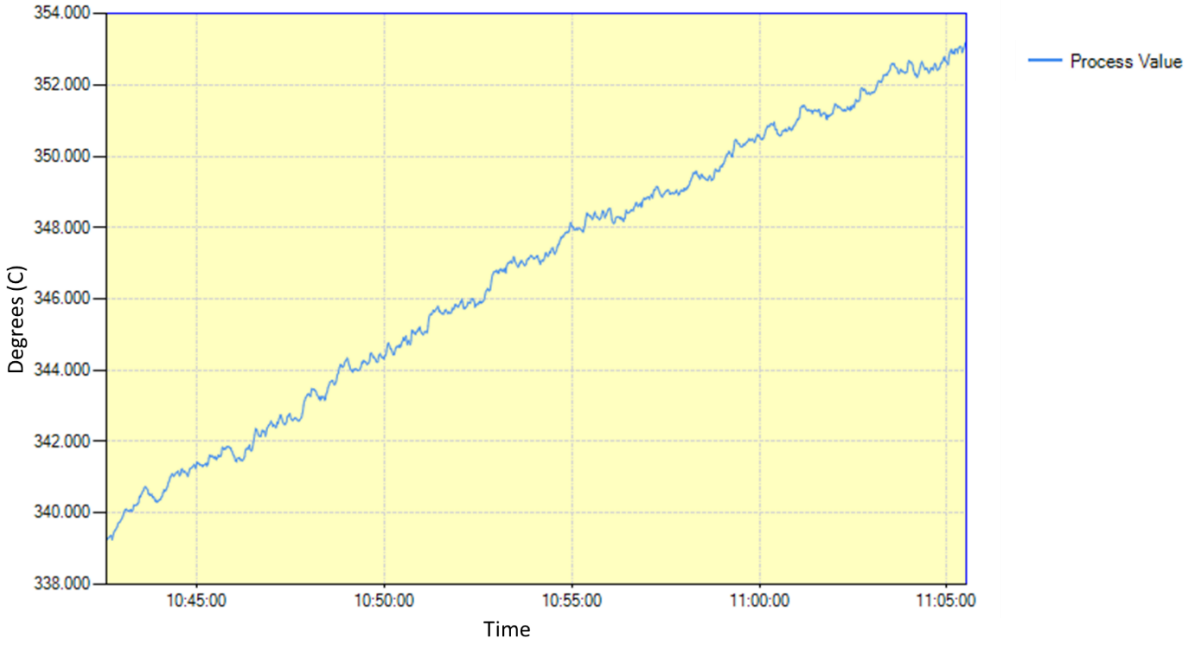

Platen temperature during 450℃ print